X 62 62964

DECLASSIFIED

CONFIDENTIAL

Copy 295

RM A54J13

NACA RM A54J13

DECLASSIFIED- US-1286
AUTHORITY- MEMO, DROBKA TO
LEBOW DATED. 6/8/66

NACA

Declassified by authority of NASA
Classification Change Notices No. 70
Dated ** 7/20/66

RESEARCH MEMORANDUM

EXPERIMENTAL INVESTIGATION OF A BODY FLARE FOR OBTAINING PITCH STABILITY AND A BODY FLAP FOR OBTAINING PITCH CONTROL IN HYPERSONIC FLIGHT

By A. J. Eggers, Jr., and Clarence A. Syvertson

Ames Aeronautical Laboratory
Moffett Field, Calif.

CASE FILE COPY

CLASSIFIED DOCUMENT

This material contains information affecting the National Defense of the United States within the meaning of the espionage laws, Title 18, U.S.C., Secs. 793 and 794, the transmission or revelation of which in any manner to an unauthorized person is prohibited by law.

NATIONAL ADVISORY COMMITTEE
FOR AERONAUTICS

WASHINGTON
January 18, 1955

37

CONFIDENTIAL

DECLASSIFIED

DECLASSIFIED
CONFIDENTIAL

NATIONAL ADVISORY COMMITTEE FOR AERONAUTICS

RESEARCH MEMORANDUM

EXPERIMENTAL INVESTIGATION OF A BODY FLARE FOR OBTAINING PITCH STABILITY AND A BODY FLAP FOR OBTAINING PITCH CONTROL IN HYPERSONIC FLIGHT

By A. J. Eggers, Jr., and Clarence A. Syvertson

SUMMARY

The effectiveness of a body flare as a pitch-stabilizing device and a body flap as a pitch-control device has been investigated experimentally at Mach numbers from 3.00 to 6.25. The basic test body was rotationally symmetric and consisted of a fineness ratio 3 nose followed by a fineness ratio 9 afterbody. The body flare was conical and was added at the base. The body flap consisted of a deflectable section of the surface of the cylindrical afterbody. This section was 1.59 body diameters long, 78° of arc in circumferential extent, and was centered 8.5 body diameters aft of the nose. Tests were conducted at angles of attack from -25° to +25° and flap deflection angles of 0°, -10°, and -25°.

Experimentally determined increments in lift and drag due to flap deflection are compared at a Mach number of 5 with the predictions of the generalized shock-expansion theory and Newtonian impact theory. Both theories are in reasonably good agreement with experiment at small angles of attack. The trim lift coefficients and lift-drag ratios of the test configuration are found to increase steadily with increasing Mach number, becoming greater than those of a comparable all-movable-wing control at the higher Mach numbers of the tests. The body flare and flap have, then, the attractive possibility at high supersonic airspeeds of providing stability and control in pitch, while at the same time they should be less vulnerable than planar airfoils to aerodynamic heating.

INTRODUCTION

The design of aircraft suitable for flight at high supersonic airspeeds is in substantial part dictated by considerations of aerodynamic heating. Aerodynamic heating is governed by many factors, including the Mach number and Reynolds number of flight and, of course, the shape of

CONFIDENTIAL

the aircraft. It is hardly to be expected that, in general, the dependence of aerodynamic heating on shape will be simple; however, it seems reasonable to anticipate that within certain limits, reducing the surface area will reduce the aerodynamic heating. Provided this is the case, it follows that the amount of surface subject to aerodynamic heating should be kept to a minimum. Especially is this true of such surfaces as present unusually severe cooling problems. In the latter category fall the thin planar surfaces normally used for lifting, stabilizing, and controlling aircraft in flight. At high supersonic airspeeds there is considerable evidence, both theoretical and experimental (see, e.g., refs. 1, 2, 3, and 4), that lift may be developed on a fuselage in sufficient quantity and at low enough drag penalty to greatly reduce, if not altogether eliminate, the need for wings. It remains to be determined whether planar surfaces for stabilizing and controlling hypersonic flight can also be largely eliminated or replaced by surfaces less vulnerable to aerodynamic heating.

Two such surfaces, one designed to provide stability in pitch, and the other to provide control in pitch, were therefore studied experimentally. The purpose of this paper is to report on the results of this preliminary investigation, and especially to determine whether or not these surfaces have promise and, hence, warrant further consideration. The stabilizing surface consisted of a conical flare located at the base of the test body. The control consisted of a deflectable section of the surface of the body and is termed a body flap. Force and moment characteristics were obtained for several flap deflections at Mach numbers from 3.00 to 6.25. Experimentally determined forces due to flap deflection are compared with predictions of theory, and flap trim effectiveness is compared with that of a corresponding low-aspect-ratio all-movable control.

SYMBOLS

A cross-sectional area of cylindrical section of test body, sq in.

C_D drag coefficient, $\frac{D}{qA}$

C_L lift coefficient, $\frac{L}{qA}$

C_N normal-force coefficient, $\frac{\text{normal force}}{qA}$

C_m pitching-moment coefficient (moment about body nose), $\frac{\text{moment}}{qAl}$

D drag, lb

d	diameter of cylindrical section of test body, in.
f	fineness ratio
L	lift, lb
l	length of test body, in.
l_n	length of nose section of test body, in.
M	Mach number
q	dynamic pressure, lb/sq in.
r	radial coordinate, in.
X	longitudinal coordinate, in.
$\overline{X}$	center of pressure (measured from nose), fraction of l
α	angle of attack, deg
δ	control deflection angle (positive for trailing edge deflected downward), deg

EXPERIMENT

Test Apparatus and Methods

The tests were conducted in the Ames 10- by 14-inch supersonic wind tunnel at Mach numbers of 3.00, 4.23, 5.05, and 6.25. For a detailed description of this wind tunnel and its aerodynamic characteristics see reference 5. Lift, drag, and pitching moment were measured with a three-component strain-gage balance. The balance system measured forces parallel and perpendicular to the balance axis and these forces were, in turn, resolved to give the lift, drag, and normal forces. Pitching moments were measured about the body base. Angles of attack up to 5° were obtained by rotating the model-balance assembly. In order to obtain angles of attack greater than 5°, bent-sting model supports were employed. All sting supports were shrouded from the air stream to within about 0.040 inch of the model base, thereby eliminating, for all practical purposes, all aerodynamic loads on the sting.

Base pressures were measured in all tests and the lift and drag components of the resultant base force (referred to free-stream static

pressure) were subtracted from measured total lift and drag forces to obtain the aerodynamic forces acting on the portions of test models ahead of the base.

Wind-tunnel calibration data (see ref. 5) were employed in combination with stagnation pressures measured with a Bourdon pressure gage to obtain the stream static and dynamic pressures of the tests. Reynolds numbers based on the diameter of the cylindrical portion of the models were

Mach number	Reynolds number, million
3.00	0.78
4.23	.72
5.05	.35
6.25	.15

Models

The models tested in the present investigation are shown in figure 1 along with a sketch giving pertinent over-all dimensions. The first model consisted of a 1-inch-diameter basic body made up of a fineness ratio 3, 3/4-power nose[1] faired into a fineness ratio 9 cylindrical afterbody. The second model consisted of the basic body modified by a conical flare at the base. This flare was a frustum of a fineness ratio 3 cone. It extended 1.242 body diameters forward of the base and increased the base diameter by $\sqrt{2}$. The third model was essentially the same as the second, with the exception that a body flap 1.590 body diameters long and 78° of arc in circumferential extent was added forward of the conical flare. This flap was centered at a station 8.5 body diameters from the nose. It had a projected lateral dimension equal to 0.629 body diameter and a plan area equal to the square of the body diameter. This particular configuration was chosen because it was desired to compare the data obtained for the flap with those obtained for an all-movable-wing model. This latter model, which was tested in the Ames 10- by 14-inch wind tunnel in conjunction with a separate research program, consisted of the same basic body, with a rectangular plan form, all-movable control of aspect ratio 4/9 (for the exposed panels joined together). The control was also centered 8.5 body diameters from the nose and had the same plan area as the body flap. The chord of the control was equal to 1.5 body diameters, and the exposed semispan was equal to 1/3 body diameter. A 4-percent-thick, biconvex airfoil section with a 50-percent-blunt trailing edge was employed.

[1]Specifically, this nose is defined by the relation $r = \frac{d}{2}(x/l_n)^{3/4}$ and was chosen to provide a basic body of lower than average minimum drag (see refs. 3 and 6).

Neither the body-flap model nor the all-movable-wing model is intended to represent a practical aircraft configuration. Nevertheless, these models provide experimental results on the relative merits of the body-flap configuration.

Accuracy of Test Results

Stream Mach numbers did not vary more than ±0.02 from the mean values of 3.00, 4.23, and 5.05. A maximum variation of ±0.04 existed at the peak test Mach number of 6.25. Stream Reynolds number for a given Mach number did not depart by more than ±10,000 from the mean values given in the section "Test Apparatus and Methods."

The over-all accuracy in angle-of-attack values, including uncertainties in the corrections for stream angle and for deflections of the model support, is estimated to be $\pm 0.2^{\circ}$.

Uncertainties in the measurement of forces acting on the models and in the determination of free-stream dynamic pressures influenced the accuracy of computed force coefficients. At angles of attack up to 10° and Mach numbers up to 5, these uncertainties resulted in maximum estimated errors in lift, drag, and normal-force coefficients of ±0.015. A corresponding error of ±0.030 is estimated at Mach number 6.25. At angles of attack in excess of 10°, the error increases to ±0.020 at Mach numbers up to 5 and ±0.045 at Mach number 6.25. Pitching-moment coefficients are estimated to be in error by not more than ±0.020, except at Mach number 6.25 where the value is ±0.045. Finally, it should be emphasized that, for the most part, the experimental results presented herein are in error by less than these estimates.

RESULTS AND DISCUSSION

All the experimental data for the three models tested during the investigation are presented in table I. Typical data are also presented in graphical form in figures 2 through 4. In analyzing these results, it is convenient to consider first the effectiveness of the conical flare in stabilizing the basic body.

Stability of Flared Body

Conical flares similar to the one tested here have been investigated previously (see, e.g., ref. 7), though the intent was not to reduce the

severity of problems associated with aerodynamic heating. The size of the conical flare used in the present tests was fixed by requiring that the center of pressure on the body be shifted slightly aft of the midship location.[2] According to Newtonian impact theory the center of pressure of the flared body was nearly constant with changes in angle of attack, ranging from 56 percent of the body length aft of the nose at $\alpha=0^{\circ}$ to 57 percent at $\alpha=25^{\circ}$. The experimentally determined centers of pressure are shown in figure 5 and are compared with those of the basic body.[3] It is seen that the flare is effective both in moving the center of pressure of the basic body aft and in reducing its travel with angle of attack. At the lower Mach numbers and angles of attack, the center of pressure is somewhat ahead of that estimated with impact theory. At the highest Mach number, however, the estimate of 56 to 57 percent is apparently too low. Center-of-pressure results are also shown for the body with wing. It is seen that whereas the effectiveness of the conical flare increases with Mach number, the effectiveness of the wing decreases (as might be expected from thin-airfoil theory), becoming generally inferior to that of the flare at Mach numbers in the nieghborhood of 5 and greater. Movement of the wing to a more rearward location would no doubt shift the center of pressure aft; however, the effect of Mach number on the ability of the wing to fix center of pressure would seem likely to remain essentially the same. Certainly, the experimental results do confirm the prediction that a conical flare may be employed to provide pitch stability to a body in hypersonic flight. It should also be noted that this stability is achieved with little change in lift-drag ratio at Mach numbers greater than 5 since the flare increases both the lift and drag of the body in approximately the same proportions (see figs. 2 and 3).

Effect of Body Flap on Lift and Drag

Deflection of the body flap influences the force characteristics of the flared body as shown in figure 6 where the variations of C_L and C_D with flap deflection at various angles of attack and Mach numbers are presented. Examination of these results shows that the present body flap is not an especially powerful control. Reasonable flap effectiveness is attained, however, at low angles of attack for the higher flap deflections.

[2]With this provision, plus the assumption that the cone of which the flare is a frustum should have the same fineness ratio as the nose (f=3), it was indicated by Newtonian impact theory (see, e.g., ref. 8) that the normal-force contribution of the flared section should be the same as that of the nose section. In consequence of these conditions, the base diameter of the conical flare is just $\sqrt{2}$ times the diameter of the basic body.

[3]The results presented for center of pressure were obtained graphically in the usual manner from data (see tables I(a) and (b)) on C_m and C_N.

Evidently, too, this effectiveness is fairly independent of Mach number. At high positive angles of attack the flap is essentially ineffective. On the other hand the flap remains effective at large negative angles of attack. This result suggests that the body-flap control might be most effective in a canard configuration - one, for example, like the nose flap investigated independently by Lazzeroni (ref. 9) at lower supersonic speeds. The nose flap was designed, however, with a different objective in mind; namely, it was intended to provide pitch control for a missile airframe having small lateral dimensions. It seems likely, however, that a canard arrangement or, for that matter, almost any arrangement with the flap deflected on the windward side of the body would be unstable in roll. Planar fins, such as those employed in reference 9, would, of course, provide roll damping.[4] If stability and control are to be obtained aerodynamically in the absence of planar surfaces, the body flap should be located aft on what is normally the lee side of the body - that is, in a position something like the one used in the present investigation. In this event, however, the flap does not, in the light of the experimental data just discussed, appear promising for application at high angles of attack.

Trim Conditions

The body flap deflected -25° influences the center of pressure as shown in figure 7. Results are also shown for the flared body with flap undeflected. By assuming a reasonable static margin, we can determine the trim lift coefficients for the flared body with flap over the Mach number range. If a static margin equal to 3 percent of the body length at $\alpha=0^{\circ}$ is taken and the results of figure 7 are used, these lift coefficients are found to vary with Mach number as shown in figure 8. Variation of the corresponding coefficients for the model with all-movable wing deflected -25° is also shown. It is seen that the lift coefficients at trim for the body-flap model increase steadily with Mach number. In contrast to this result, the trim lift coefficients for the model with all-movable wing decrease markedly with Mach number, falling below those of the body-flap model at the highest Mach number.

The lift-drag ratios corresponding to these trim lift coefficients are shown in figure 9 for the two configurations. The trends observed in the lift-drag ratios also favor the body-flap model at the higher test Mach numbers.[5]

[4]While the addition of such fins may present no problem at low supersonic speeds, their addition would lead to aerodynamic-heating problems at high supersonic speeds, tending to defeat the advantage sought here with the present body-flap configuration.

[5]The maximum trim lift-drag ratios attainable with each control at the various test Mach numbers might make a better comparison. However, due to the limited number of control deflections tested in the present investigation, it was not possible to determine these quantities accurately.

Up to now we have considered, so to speak, only the gross effects of a conical flare and body flap on the aerodynamic characteristics of a body of revolution. In the interests of better understanding how these devices influence flow about the body, it is appropriate next to discuss results of flow visualization studies.

Flow Visualization Studies

Two types of study were made. First, shadowgraph pictures were taken of the flow in the region of the flap and flare at Mach numbers of 4.23, 5.05, and 6.25. The model was set at 0° angle of attack with flap deflections of -10° and -25°. (Note the model was moved downstream in the tunnel to permit the taking of these pictures.) Second, the flow at the surface was observed at a Mach number of 4.23 using the China-clay technique[6] (see, e.g., ref. 10). Typical results of these studies are presented in figure 10. It is indicated by the shadowgraph pictures that the shock wave produced by the flap has caused only moderate thickening of the boundary layer forward of the flap. The China-clay pictures verify this point and show further that the boundary layer tends to bleed around the sides of the flap from the high-pressure region on the top to the low-pressure region below and behind. Much the same phenomenon has been observed in studies of boundary-layer flow over ramps in front of inlets (see ref. 11). Accordingly, shock-wave-boundary-layer interaction would not appear to play an important role in the performance of the body flap, at least at intermediate to large angles of deflection.

The flow aft of the flap is apparently separated, however, as is strikingly indicated by the absence of a strong shock wave emanating from the upper part of the conical flare (see figs. 10(a) and (b), $M = 4.23$) and by the streamline pattern in the China-clay pictures. This flow separation may be expected to reduce the forces on the tail cone and should, of course, be considered in any calculation of flap effectiveness.

With these points in mind, it is undertaken next to determine how well flap characteristics can be predicted by theory.

Comparison of Theory and Experiment

A limited number of calculations have been made to estimate the incremental force coefficients due to flap deflection. Both impact theory (ref. 8) and the generalized shock-expansion method (refs. 12 and 13) were

[6]It was not possible to obtain results for the higher test Mach numbers because the drying time of the fluid used in the tests was less than the time required to establish flow at these Mach numbers.

employed.[7] In these calculations, the interference of the flap on the flare was determined by considering, as prescribed by impact theory (see ref. 8), that no forces act on any part of the body shadowed from the free stream by the deflected flap.

The results of the calculations are compared with those of experiment in figure 11 for the test Mach number of 5.05 and angles of attack $+10^{\circ}$, 0°, and -10°. The predictions of both theories are generally in from fair to good agreement with the experimental results at angles of attack of 0° and -10°.[8] At $+10^{\circ}$ angle of attack, only qualitative agreement is obtained with either theory (impact theory gives zero force increments since the flap is always within the shadow of the forward part of the body). Evidently, then, neither theory properly accounts for the fact that the flap is operating largely in the wake of the body.

The effect of flap-flare interference on incremental lift coefficient is illustrated at zero angle of attack in figure 11(b) where results are shown for the coefficients calculated with impact theory neglecting interference. Comparison of these results with those including the interference indicates that the shadow concept of impact theory is adequate in this case for predicting the interference effects. These results also show that the interference has a significant detrimental influence on flap effectiveness. Recommendations for elimination of this influence will be discussed later.

CONCLUDING REMARKS AND FUTURE DESIGN CONSIDERATIONS

Results of the experimental investigation of a body of revolution having a conical flare at the base to provide stability in pitch and fitted with a body flap to provide control in pitch have been analyzed at Mach numbers from 3 to 6.25. It was found that these devices do, in fact, perform their intended function at high supersonic airspeeds. In particular, the conical flare was effective in fixing the center-of-pressure location slightly aft of the midship point on the body at Mach numbers in excess of 4 and angles of attack up to 25°. The body flap improved as a trim device over the Mach number range of the tests. At Mach numbers in excess

[7]The initial conditions for the shock-expansion solutions were determined from pressure distributions (and shock waves) measured for a cone having a semivertex angle of 18.93°. (These data were obtained in conjunction with an independent series of tests in the 10- by 14-inch supersonic wind tunnel.) The use of this procedure means, in effect, that for the purposes of these calculations, the blunt nose of the body was replaced with a cone tangent to the 3/4-power profile at 1.77 percent of the nose length.

[8]One exception, that for the incremental lift coefficient at $\alpha=-10^{\circ}$ and $\delta=-10^{\circ}$, is noted. Although the cause of this difference between theory and experiment is not known, it is believed that it is due to a more extensive and complex interference than considered by the theories.

of about 5, the combination of body flap and conical flare became superior to an all-movable wing, providing larger trim lift coefficients and larger trim lift-drag ratios at a control deflection of -25°. These results offer encouragement to the possibility of designing stable and controllable hypersonic aircraft essentially free of planar surfaces which present inordinately severe aerodynamic-heating problems.

Experimentally determined increments in lift and drag due to flap deflection were compared at a Mach number of 5 to the predictions of both the generalized shock-expansion method and the Newtonian impact theory. The predictions of both theories were found to be in fair to good agreement with experimental results at small angles of attack. In the application of the theories, it was found that consideration must be given to the interference of the flap on the conical flare. This finding was brought out and supported by a series of visual studies of the flow in the region of the flap and flare.

In general, the effectiveness of the flap as employed in these tests was found to be low at small flap deflections and, more or less irrespective of flap deflection, at large positive angles of attack (in the neighborhood of 20°). It seems unlikely that flaps of this type located on the lee side of a body offer much promise of being made effective at large angles of attack, inasmuch as under these circumstances the flap is largely submerged in the wake of the body. Flap effectiveness for small flap deflections may, however, be improved over that obtained in the present tests by locating the flap on a positively inclined surface rather than on the cylindrical afterbody, such as was done here. The conical flare provides a logical surface for this purpose since this location of the flap will have the added advantage of eliminating the unfavorable effects of flap-flare interference. The resulting configuration might appear something like that shown in figure 12, though, of course, many variations are possible. This configuration has the same over-all fineness ratio as the test body of this report, but it has a more slender nose and stabilizing cone. This modification should, of course, increase the attainable lift-drag ratios (see ref. 4). The body flap could be employed in pairs rather than singly, thereby permitting an increase in over-all effectiveness at small and intermediate flap deflections by allowing the lower or windward flap to be retracted into the flare while the leeward flap is extended away from the flare. Retraction of the lower or windward flap would, in effect, reduce the stabilizing effect of the tail cone and thereby permit a further increase in trim lift. It is noticed, too, that a pair of yaw control flaps has been incorporated in this design, the assumption being that if the body flap is effective in pitch, it should also be effective in yaw.[9] It is, of course, a logical extension of this control to consider the all-movable tail cone. Also, it is observed that some stability

[9]Simultaneous deflection of all four flaps would also provide a method of controlling the body center-of-pressure location and, hence, controlling the stability of the configuration.

in roll should be provided by the extended flap. These possibilities must, of course, be investigated experimentally to determine the extent to which they can actually be realized.

Ames Aeronautical Laboratory
National Advisory Committee for Aeronautics
Moffett Field, Calif., Oct. 13, 1954

REFERENCES

1. Sänger, Eugene: Raketen-flugtechnik. R. Oldenbourg (Berlin), 1933, pp. 112, 120-121.

2. Resnikoff, Meyer M.: Optimum Lifting Bodies at High Supersonic Airspeeds. NACA RM A54B15, 1954.

3. Dennis, David H., and Cunningham, Bernard E.: Forces and Moments on Pointed and Blunt-Nosed Bodies of Revolution at Mach Numbers From 2.75 to 5.00. NACA RM A52E22, 1952.

4. Dennis, David H., and Cunningham, Bernard E.: Forces and Moments on Inclined Bodies at Mach Numbers From 3.0 to 6.3. NACA RM A54E03, 1954.

5. Eggers, A. J., Jr., and Nothwang, George J.: The Ames 10- by 14-Inch Supersonic Wind Tunnel. NACA TN 3095, 1954.

6. Eggers, A. J., Jr., Dennis, David H., and Resnikoff, Meyer M.: Bodies of Revolution for Minimum Drag at High Supersonic Airspeeds. NACA RM A51K27, 1952.

7. Ross, F. W., and Dorrance, W. H.: An Introduction to a Supersonic Body Development Study. Univ. of Mich., Engineering Research Institute, UMM-40, Dec. 1949.

8. Grimminger, G., Williams, E. P., and Young, G. B. W.: Lift on Inclined Bodies of Revolution in Hypersonic Flow. Jour. Aero. Sci., vol. 17, no. 11, Nov. 1950, pp. 675-690.

9. Lazzeroni, Frank A.: Investigation of a Missile Airframe with Control Surfaces Consisting of Projecting Quadrants of the Nose Cone. NACA RM A53L21, 1954.

10. Gazley, Carl, Jr.: The Use of the China-Clay Lacquer Technique for Detecting Boundary-Layer Transition. Gen. Electric Co., Schenectady, N. Y. Gen. Engineering and Consulting Lab. Rep. 49A0536, 1950.

11. Davis, Wallace F., and Goldstein, David L.: Experimental Investigation at Supersonic Speeds of Twin-Scoop Duct Inlets of Equal Area. I - An Inlet Enclosing 61.5 Percent of the Maximum Circumference of the Forebody. NACA RM A7J27, 1948.

12. Eggers, A. J., Jr.: On the Calculation of Flow About Objects Traveling at High Supersonic Speeds. NACA TN 2811, 1952.

13. Eggers, A. J., Jr., and Savin, Raymond C.: Approximate Methods for Calculating the Flow About Nonlifting Bodies of Revolution at High Supersonic Airspeeds. NACA TN 2579, 1951.

DECLASSIFIED

TABLE I.- FORCE AND MOMENT CHARACTERISTICS

(a) Basic body

M	α	C_L	C_D	C_N	C_m	M	α	C_L	C_D	C_N	C_m
3.00	0	0	0.146	0	0	5.05	0	0	0.104	0	0
	2.03	.102	.158	.108	-.031		2.01	.120	.116	.124	-.039
	2.91	.167	.184	.176	-.049		2.89	.230	.132	.236	-.105
	4.94	.311	.195	.327	-.104		4.90	.401	.164	.414	-.172
	6.96	.520	.223	.544	-.187		6.91	.632	.213	.653	-.293
	10.06	.984	.332	1.027	-.420		7.90	.771	.243	.797	-.369
	13.19	1.544	.520	1.622	-.724		9.91	1.032	.325	1.072	-.509
	17.64	2.400	.914	2.564	-1.197		11.93	1.308	.431	1.368	-.660
	20.78	2.995	1.310	3.265	-1.570		18.22	2.212	.936	2.394	-1.120
	25.00	3.820	1.981	4.300	-2.125		20.25	2.552	1.154	2.794	-1.326
							22.28	2.903	1.412	3.222	-1.558
4.23	0	0	.114	0	0						
	2.02	.113	.122	.117	-.040	6.25	0	0	.117	0	0
	2.90	.189	.139	.195	-.066		2.00	.108	.126	.112	-.040
	4.92	.352	.154	.364	-.134		2.88	.189	.133	.196	-.083
	6.94	.609	.197	.629	-.274		4.89	.375	.172	.388	-.189
	7.94	.755	.227	.779	-.341		6.89	.528	.211	.549	-.257
	9.97	1.033	.310	1.071	-.482		7.87	.722	.235	.747	-.368
	12.01	1.328	.418	1.385	-.634		9.88	.951	.290	.987	-.504
	18.38	2.333	.934	2.509	-1.206		11.89	1.181	.390	1.237	-.653
	20.44	2.698	1.173	2.938	-1.434		18.13	1.888	.826	2.052	-.939
	22.49	3.041	1.440	3.360	-1.657		20.14	2.202	1.040	2.425	-1.150
							22.15	2.564	1.319	2.872	-1.389

(b) Flared body; δ = 0°

M	α	C_L	C_D	C_N	C_m	M	α	C_L	C_D	C_N	C_m
3.00	0	0	0.270	0	0	5.05	0	0	0.163	0	0
	2.04	.148	.281	.158	-.070		2.01	.189	.189	.190	-.097
	2.91	.222	.297	.237	-.110		2.90	.326	.204	.336	-.194
	4.95	.396	.310	.421	-.196		4.91	.564	.234	.581	-.330
	6.99	.630	.326	.665	-.317		6.92	.825	.292	.854	-.480
	10.08	1.112	.460	1.176	-.557		7.91	.922	.352	.961	-.514
	13.22	1.738	.659	1.842	-.923		9.93	1.209	.451	1.269	-.673
	17.69	2.723	1.174	2.951	-1.561		11.95	1.525	.587	1.613	-.871
	20.85	3.384	1.652	3.751	-2.061		18.24	2.601	1.042	2.797	-1.517
	24.01	4.058	2.128	4.567	-2.573		20.26	2.997	1.333	3.273	-1.823
							22.30	3.416	1.729	3.816	-2.156
4.23	0	0	.207	0	0						
	1.01	.078	.211	.082	-.044	6.25	0	0	.140	0	0
	2.02	.151	.216	.158	-.078		2.00	.191	.155	.211	-.121
	7.95	.887	.326	.924	-.472		2.89	.318	.175	.326	-.224
	9.99	1.183	.419	1.237	-.628		4.89	.532	.207	.549	-.342
	12.03	1.512	.546	1.593	-.824		6.90	.730	.256	.756	-.457
	18.41	2.705	1.168	2.944	-1.632		7.88	1.039	.297	1.070	-.650
	20.47	3.098	1.467	3.415	-1.898		18.03	2.376	1.201	2.631	-1.546
	22.52	3.508	1.790	3.906	-2.179		20.15	2.715	1.475	3.056	-1.814
							22.16	2.907	1.759	3.356	-1.894

(c) Body-flap model; δ = -10°

M	α	C_L	C_D	C_N	C_m	M	α	C_L	C_D	C_N	C_m
3.00	-24.01	-4.024	2.260	-4.595	2.513	5.05	-22.30	-3.387	1.902	-3.856	2.137
	-20.85	-3.348	1.702	-3.735	1.969		-20.27	-3.007	1.563	-3.363	1.847
	-17.68	-2.687	1.250	-2.940	1.521		-18.24	-2.628	1.269	-2.893	1.580
	-12.17	-1.545	.670	-1.651	.798		-11.95	-1.548	.640	-1.647	.876
	-10.08	-1.117	.531	-1.193	.541		-9.92	-1.212	.499	-1.280	.661
	-8.00	-.747	.438	-.801	.331		-7.91	-.928	.390	-.972	.496
	-7.00	-.633	.422	-.679	.307		-6.92	-.826	.344	-.862	.475
	-4.95	-.395	.387	-.427	.180		-4.91	-.560	.289	-.583	.320
	-2.92	-.232	.380	-.251	.102		-2.90	-.329	.244	-.341	.197
	-2.05	-.172	.343	-.184	.067		-2.02	-.169	.224	-.176	.057
	-1.03	-.096	.330	-.102	.030		-1.01	-.101	.214	-.104	.032
	0	-.026	.323	-.026	-.002		0	-.018	.192	-.018	-.006
	1.01	.049	.327	.054	-.037		1.01	.083	.199	.087	-.060
	2.03	.120	.322	.132	-.069		2.01	.172	.205	.179	-.104
	4.94	.353	.359	.383	-.173		2.89	.289	.227	.300	-.166
	6.98	.562	.379	.603	-.278		4.91	.500	.256	.521	-.280
	7.99	.681	.401	.731	-.316		6.92	.768	.307	.799	-.434
	10.07	1.071	.490	1.140	-.545		7.90	.904	.321	.939	-.492
	12.16	1.502	.607	1.597	-.794		9.92	1.202	.430	1.258	-.674
							11.94	1.521	.567	1.606	-.874
4.23	-22.53	-3.493	1.902	-3.955	2.190						
	-20.47	-3.117	1.570	-3.469	1.914	6.25	-22.16	-2.929	1.749	-3.373	1.864
	-18.42	-2.747	1.284	-3.012	1.698		-20.14	-2.593	1.408	-2.917	1.626
	-12.03	-1.539	.620	-1.638	.831		-18.13	-2.277	1.120	-2.513	1.387
	-9.99	-1.213	.481	-1.278	.639		-11.89	-1.402	.604	-1.497	.827
	-7.95	-.904	.384	-.949	.466		-9.88	-1.109	.466	-1.172	.626
	-6.95	-.626	.350	-.664	.284		-7.87	-.818	.361	-.860	.429
	-4.93	-.454	.285	-.477	.227		-6.90	-.714	.265	-.740	.413
	-2.91	-.282	.267	-.296	.149		-4.89	-.491	.209	-.508	.285
	-2.03	-.186	.243	-.194	.085		-2.89	-.318	.197	-.327	.212
	-1.02	-.100	.239	-.105	.041		-1.00	-.111	.169	-.114	.060
	0	-.016	.238	-.016	-.003		0	-.017	.153	-.017	.007
	1.01	.067	.241	.072	-.048		1.00	.079	.161	.082	-.046
	2.02	.142	.245	.150	-.081		2.00	.177	.186	.184	-.076
	2.90	.233	.258	.246	-.128		2.89	.287	.196	.296	-.194
	4.92	.404	.266	.427	-.209		4.89	.482	.227	.500	-.298
	6.95	.678	.304	.710	-.369		6.90	.703	.281	.731	-.433
	7.94	.876	.371	.902	-.463		7.88	.843	.267	.872	-.444
	9.98	1.115	.439	1.144	-.547		9.89	1.101	.372	1.149	-.610
	12.02	1.453	.551	1.515	-.774						

(d) Body-flap model; δ = -25°

M	α	C_L	C_D	C_N	C_m	M	α	C_L	C_D	C_N	C_m
3.00	-24.09	-4.118	2.781	-4.895	2.655	5.05	-22.32	-3.546	2.523	-4.239	2.339
	-20.92	-3.540	2.189	-4.088	2.201		-20.29	-3.246	2.183	-3.802	2.108
	-17.75	-2.929	1.707	-3.310	1.764		-18.26	-2.930	1.864	-3.367	1.873
	-13.28	-2.033	1.157	-2.245	1.181		-11.97	-1.938	1.066	-2.117	1.200
	-10.14	-1.424	.886	-1.558	.803		-9.95	-1.614	.863	-1.739	.983
	-7.06	-.989	.725	-1.071	.592		-7.93	-1.311	.701	-1.395	.802
	-5.01	-.760	.659	-.815	.459		-6.94	-1.213	.617	-1.279	.782
	-2.98	-.591	.617	-.622	.378		-4.93	-.920	.512	-.960	.602
	-2.12	-.523	.574	-.544	.349		-2.91	-.678	.451	-.700	.463
	-1.09	-.449	.561	-.459	.312		-2.03	-.544	.448	-.559	.400
	-.07	-.367	.544	-.368	.266		-1.03	-.455	.412	-.462	.351
	.95	-.292	.530	-.283	.230		-.02	-.344	.368	-.344	.282
	1.98	-.198	.513	-.180	.177		.99	-.212	.354	-.206	.197
	2.86	-.125	.524	-.099	.066		2.00	-.097	.347	-.085	.110
	4.90	.069	.506	.112	.026		2.88	.038	.346	.055	.013
	6.91	.300	.524	.361	-.089		4.90	.302	.343	.330	-.141
	10.01	.791	.616	.886	-.380		6.91	.590	.375	.631	-.308
	13.17	1.514	.792	1.654	-.829		9.92	1.115	.480	1.182	-.642
	17.65	2.630	1.264	2.890	-1.556		11.94	1.472	.595	1.563	-.863
	20.81	3.290	1.683	3.673	-1.995		18.24	2.631	1.301	2.906	-1.653
	23.98	3.933	2.136	4.461	-2.434		20.27	3.027	1.598	3.393	-1.939
							22.27	3.404	1.923	3.879	-2.235
4.23	-22.57	-3.738	2.539	-4.427	2.471						
	-20.51	-3.339	2.183	-3.893	2.152	6.25	-22.16	-3.092	2.415	-3.775	2.135
	-18.45	-2.978	1.838	-3.407	1.886		-20.15	-2.781	2.062	-3.321	1.903
	-12.08	-1.915	1.023	-2.087	1.156		-18.14	-2.508	1.762	-2.932	1.683
	-10.03	-1.576	.837	-1.697	.940		-11.91	-1.821	1.052	-1.999	1.227
	-7.99	-1.247	.690	-1.331	.741		-9.90	-1.514	.831	-1.634	1.009
	-6.99	-1.115	.623	-1.182	.696		-7.89	-1.214	.656	-1.292	.817
	-4.96	-.817	.539	-.860	.514		-6.91	-1.136	.612	-1.202	.769
	-2.94	-.625	.484	-.648	.414		-4.90	-.913	.503	-.953	.648
	-2.07	-.524	.485	-.541	.357		-2.89	-.648	.409	-.668	.471
	-1.05	-.437	.461	-.445	.309		-1.00	-.387	.331	-.393	.347
	-.04	-.341	.439	-.341	.253		0	-.264	.293	-.264	.273
	.98	-.239	.410	-.232	.193		1.00	-.116	.277	-.111	.169
	1.99	-.140	.409	-.126	.137		2.88	.140	.247	.153	-.025
	2.88	-.047	.405	-.026	.077		4.89	.427	.222	.445	-.202
	4.90	.160	.385	.193	-.026		6.90	.675	.274	.703	-.362
	7.92	.635	.435	.689	-.314		7.87	.814	.338	.852	-.481
	9.97	1.009	.509	1.082	-.549		9.88	1.057	.415	1.112	-.639
	12.01	1.393	.615	1.491	-.779		11.89	1.430	.538	1.408	-.836
	18.41	2.691	1.289	2.961	-1.664		18.13	2.310	1.135	2.549	-1.509
	20.46	3.090	1.555	3.439	-1.939		20.14	2.660	1.292	2.942	-1.735
	22.52	3.490	1.877	3.943	-2.233		22.16	3.023	1.532	3.378	-1.949

NACA

DECLASSIFIED

DECLASSIFIED

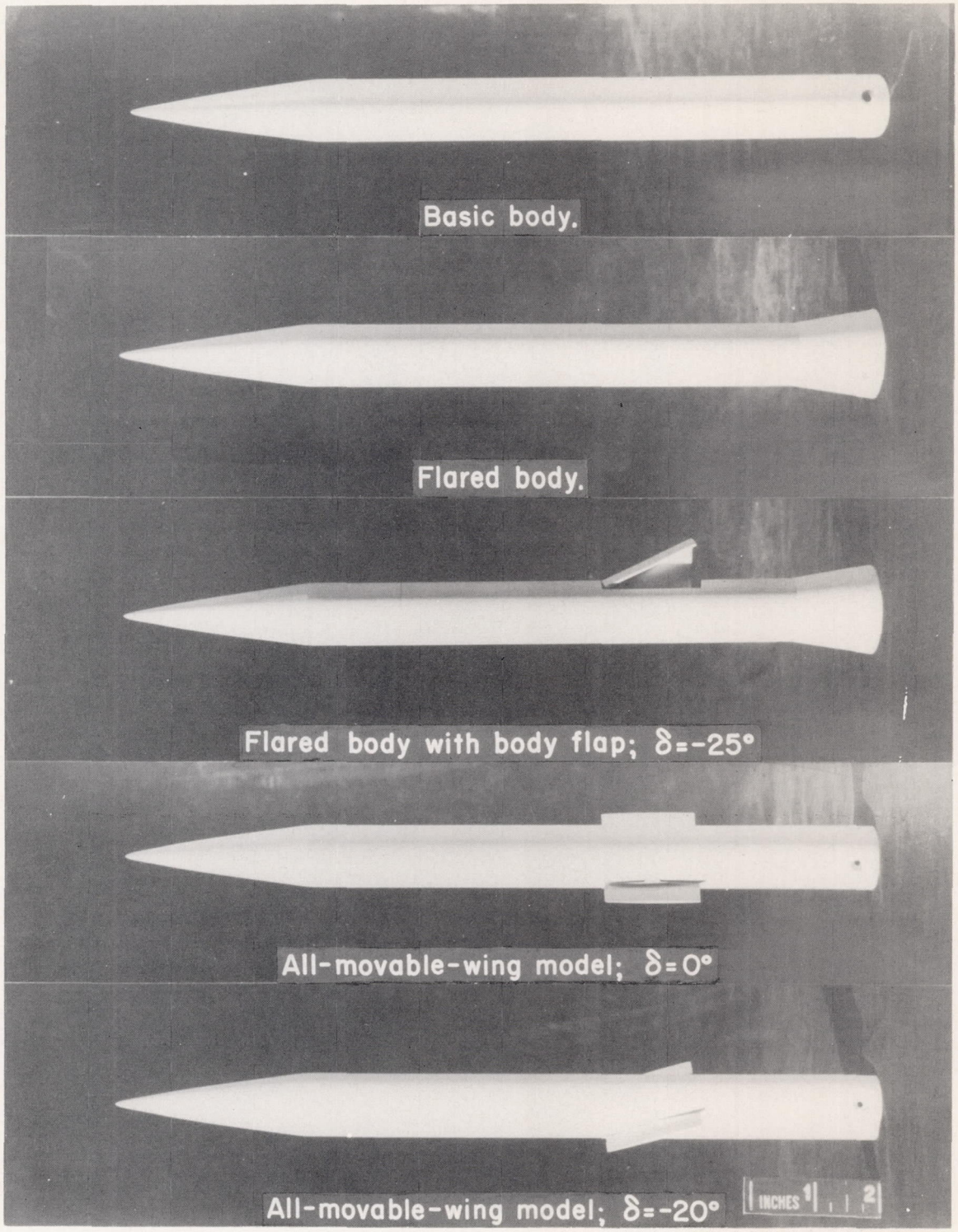

(a) Photograph of models.

A-19607

Figure 1.- Models.

CONFIDENTIAL

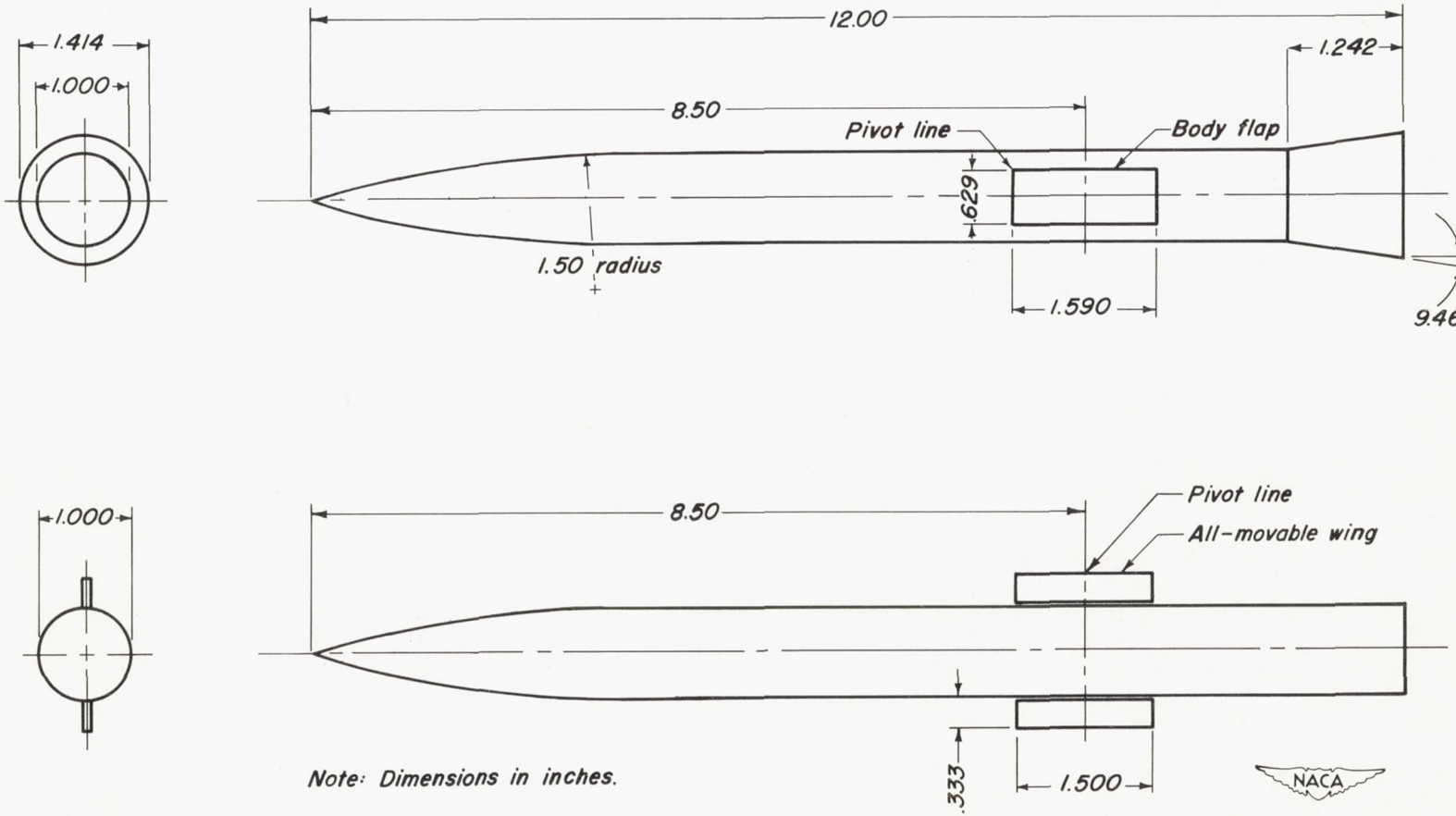

(b) Dimensioned sketch of models.

Figure 1.- Concluded.

CONFIDENTIAL

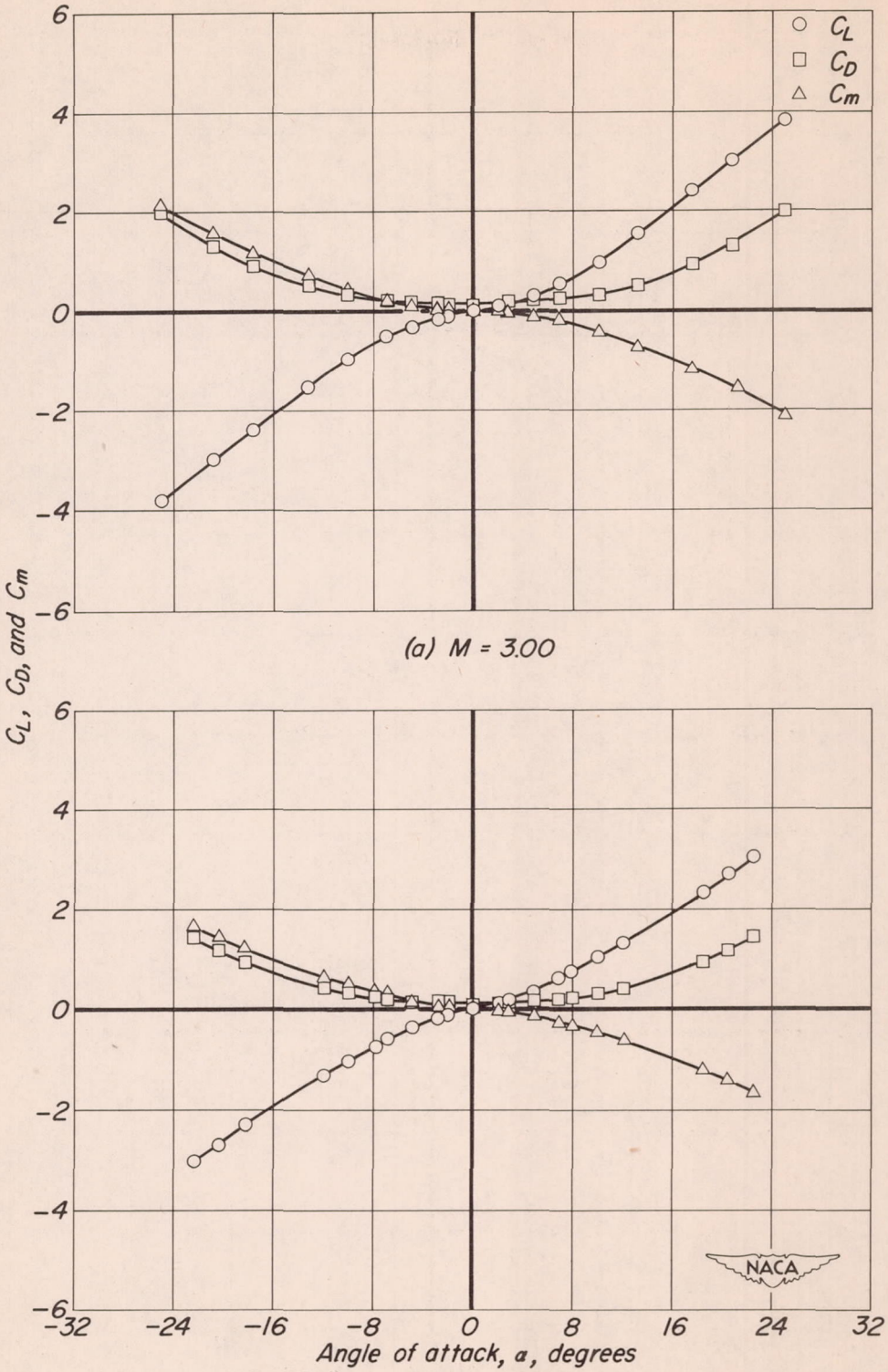

(b) M = 4.23

Figure 2.— Force and moment characteristics of basic body.

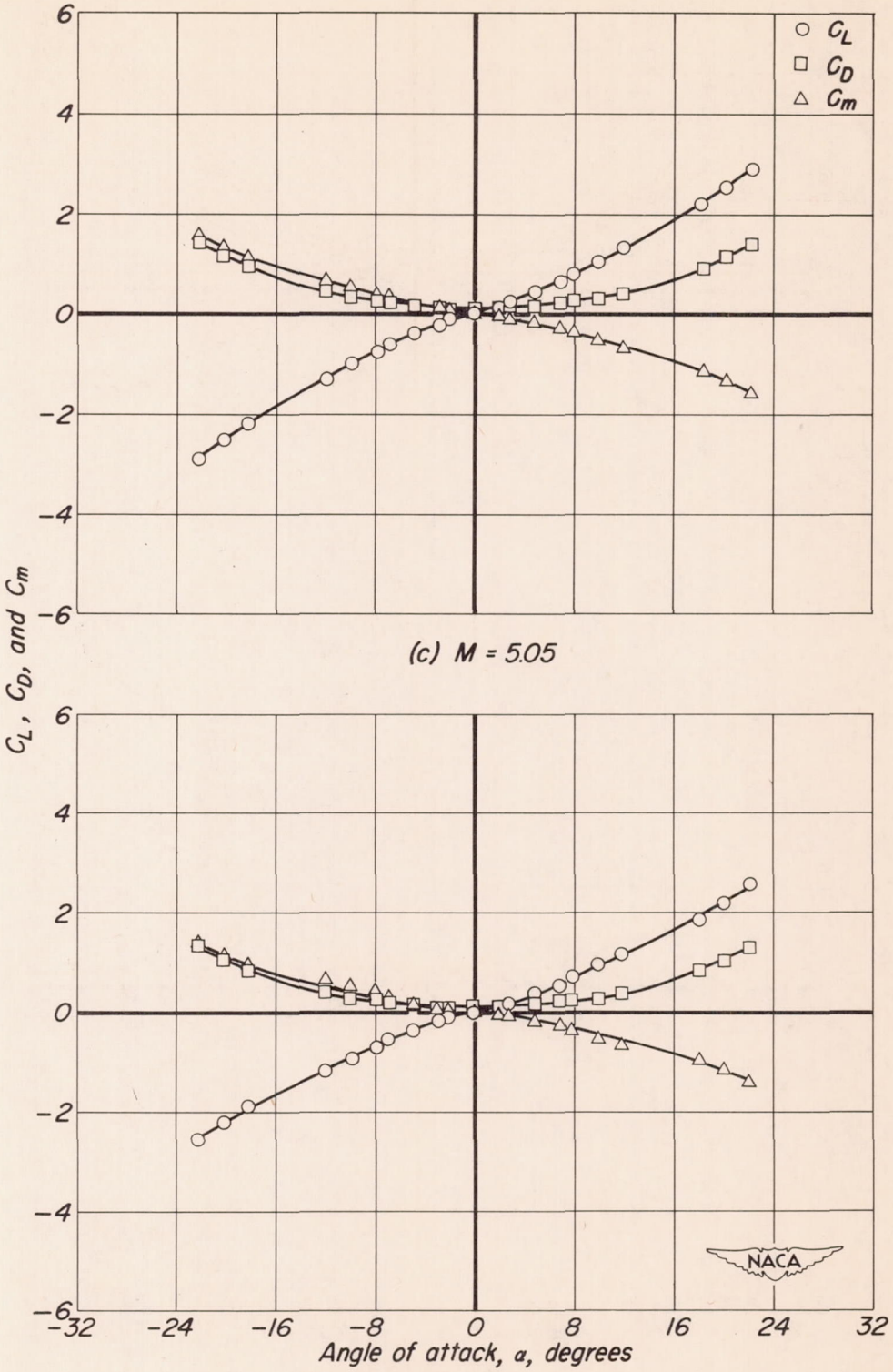

(c) M = 5.05

(d) M = 6.25

Figure 2.– Concluded.

DECLASSIFIED

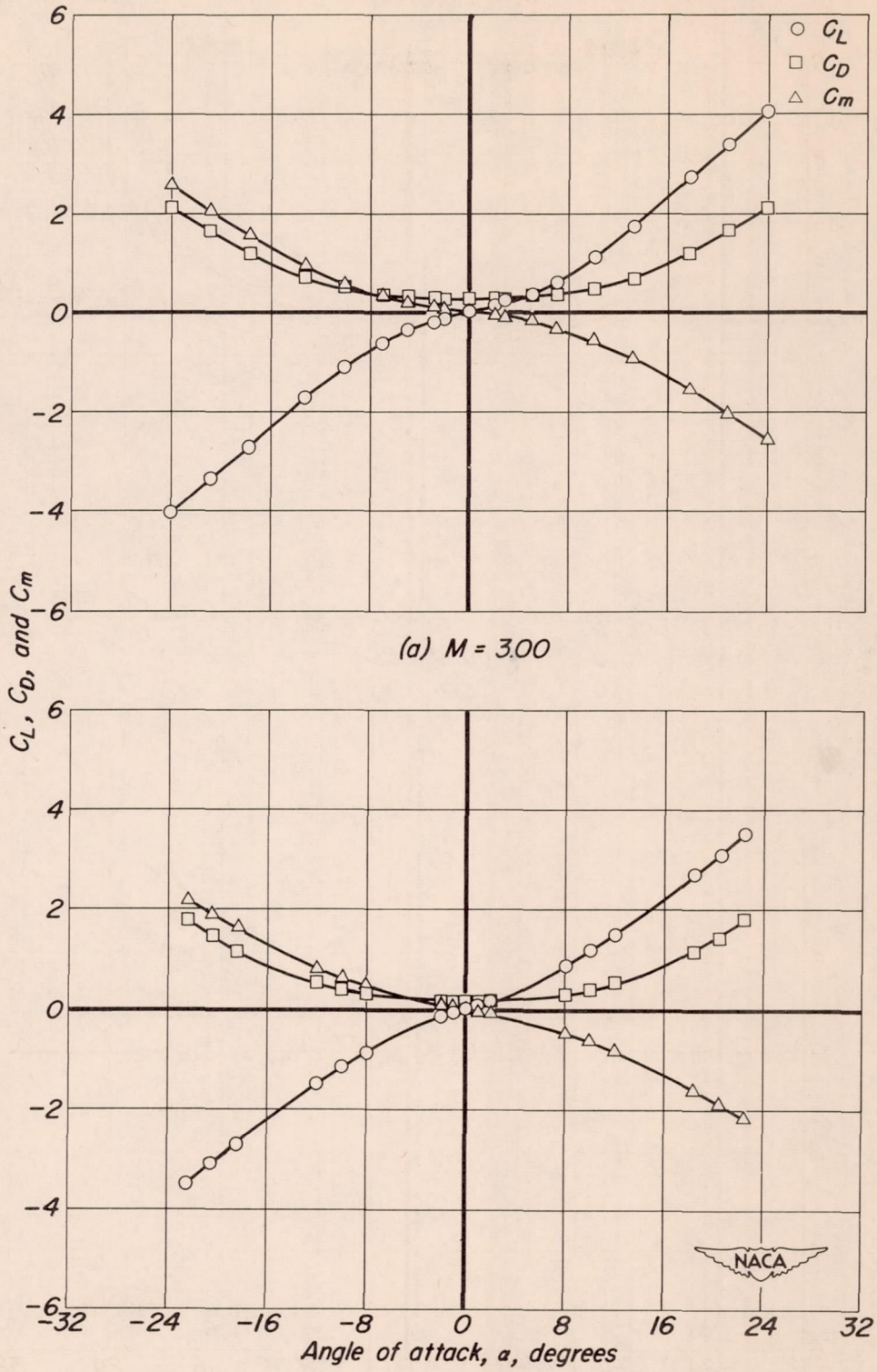

(b) M = 4.23

Figure 3.– Force and moment characteristics of body with conical flare.

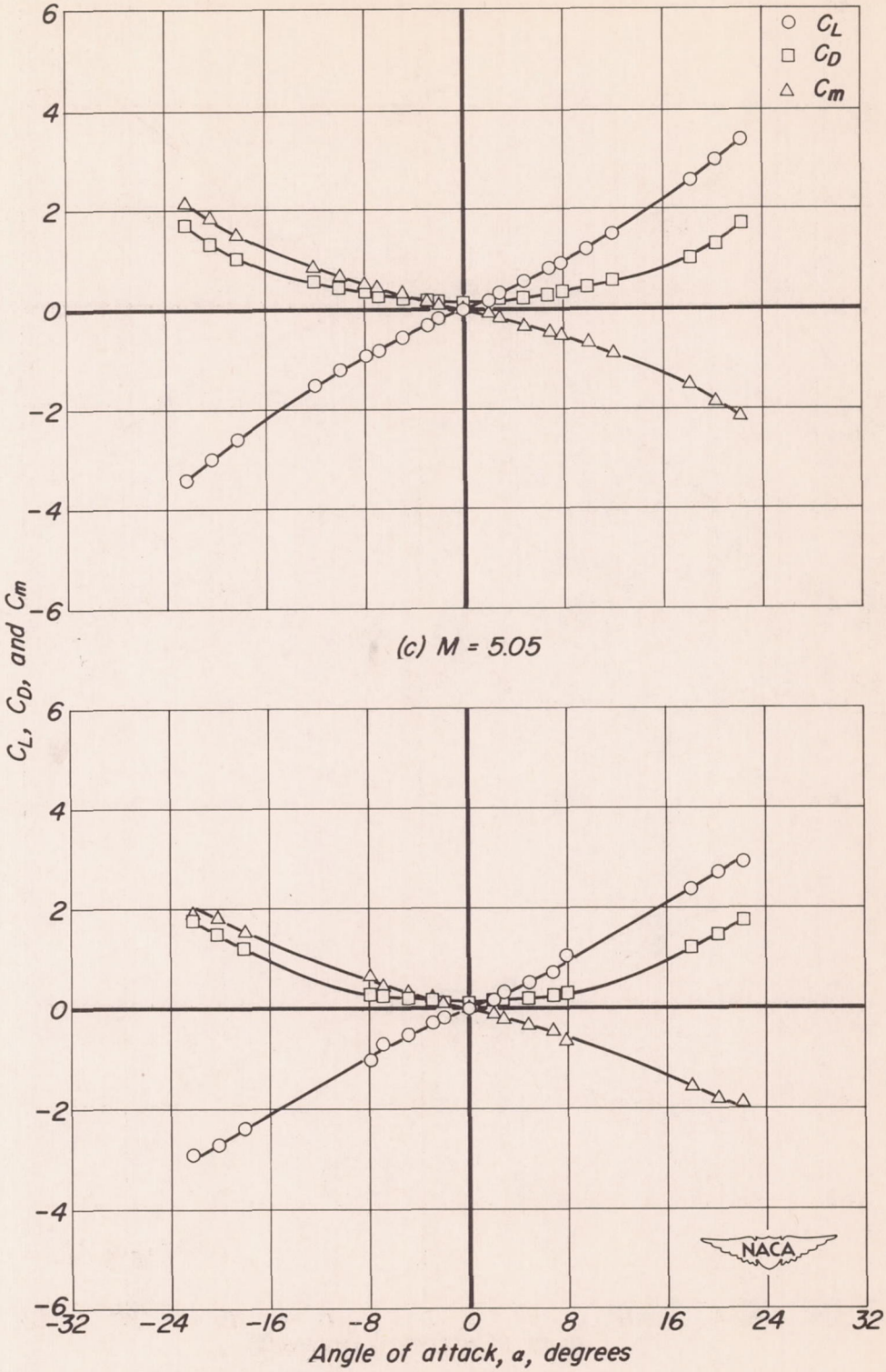

(c) M = 5.05

(d) M = 6.25

Figure 3.– Concluded.

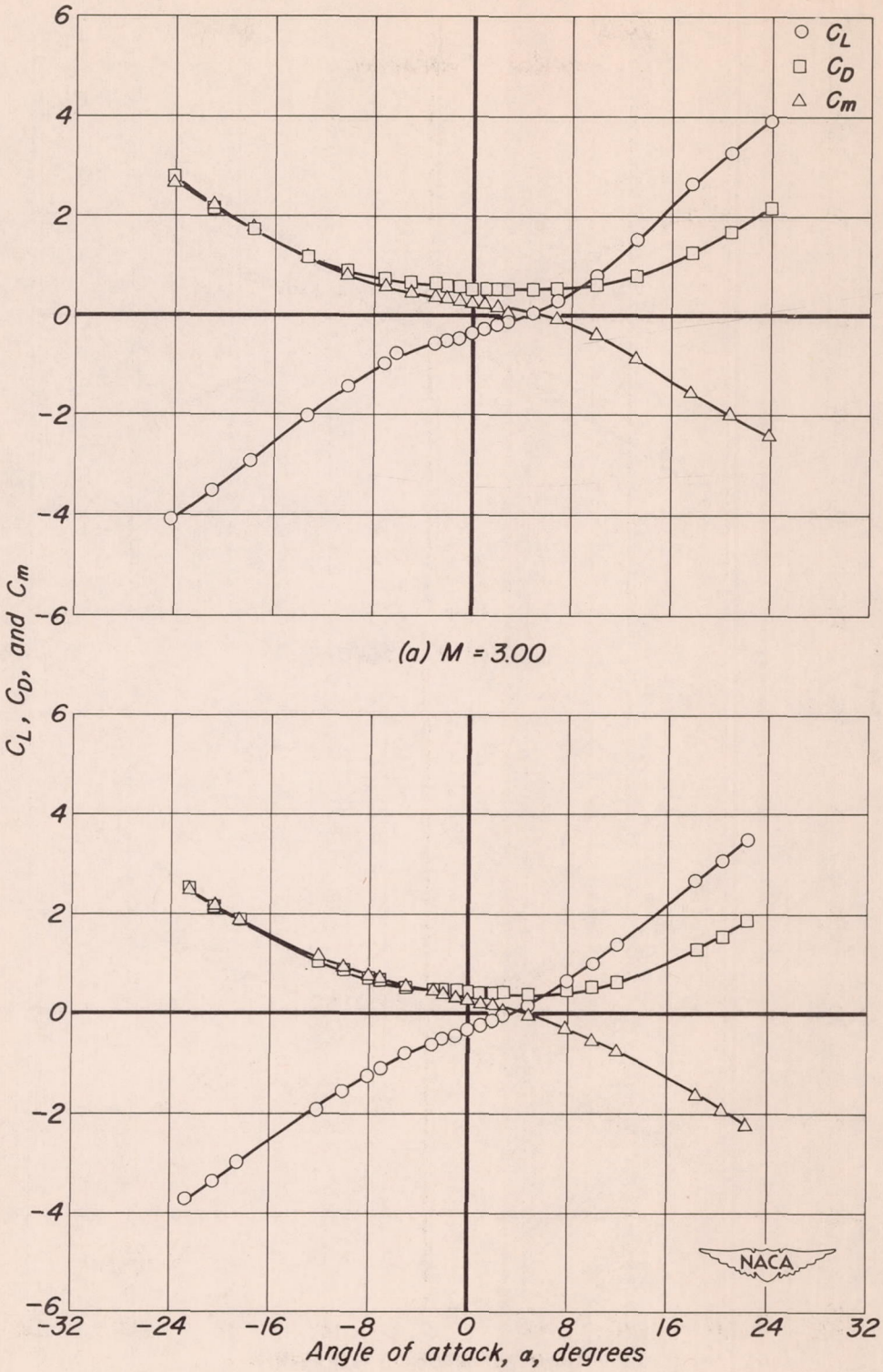

(b) M = 4.23

Figure 4.– Force and moment characteristics of body with conical flare and flap deflected −25°.

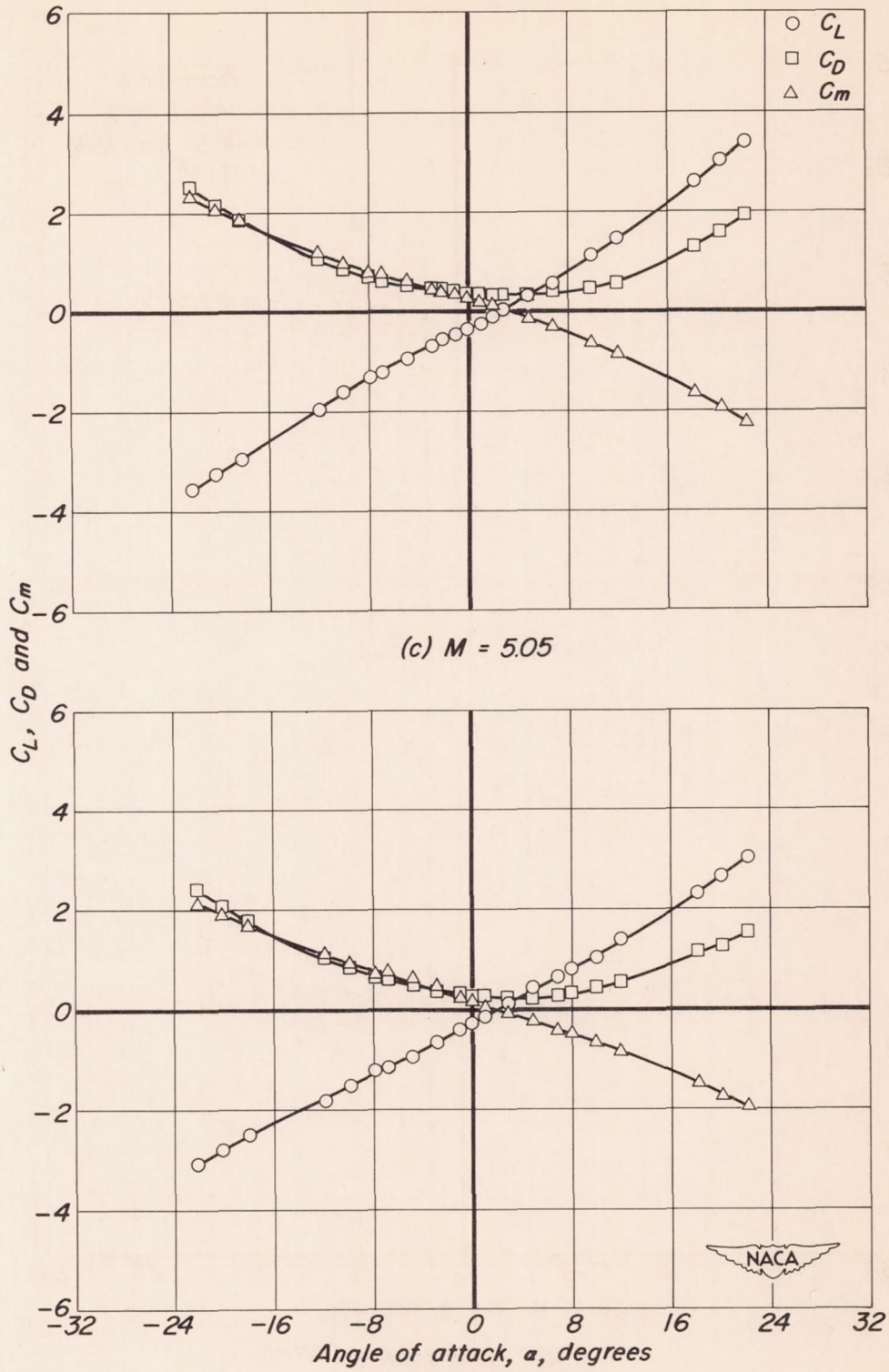

(c) M = 5.05

(d) M = 6.25

Figure 4.– Concluded.

DECLASSIFIED

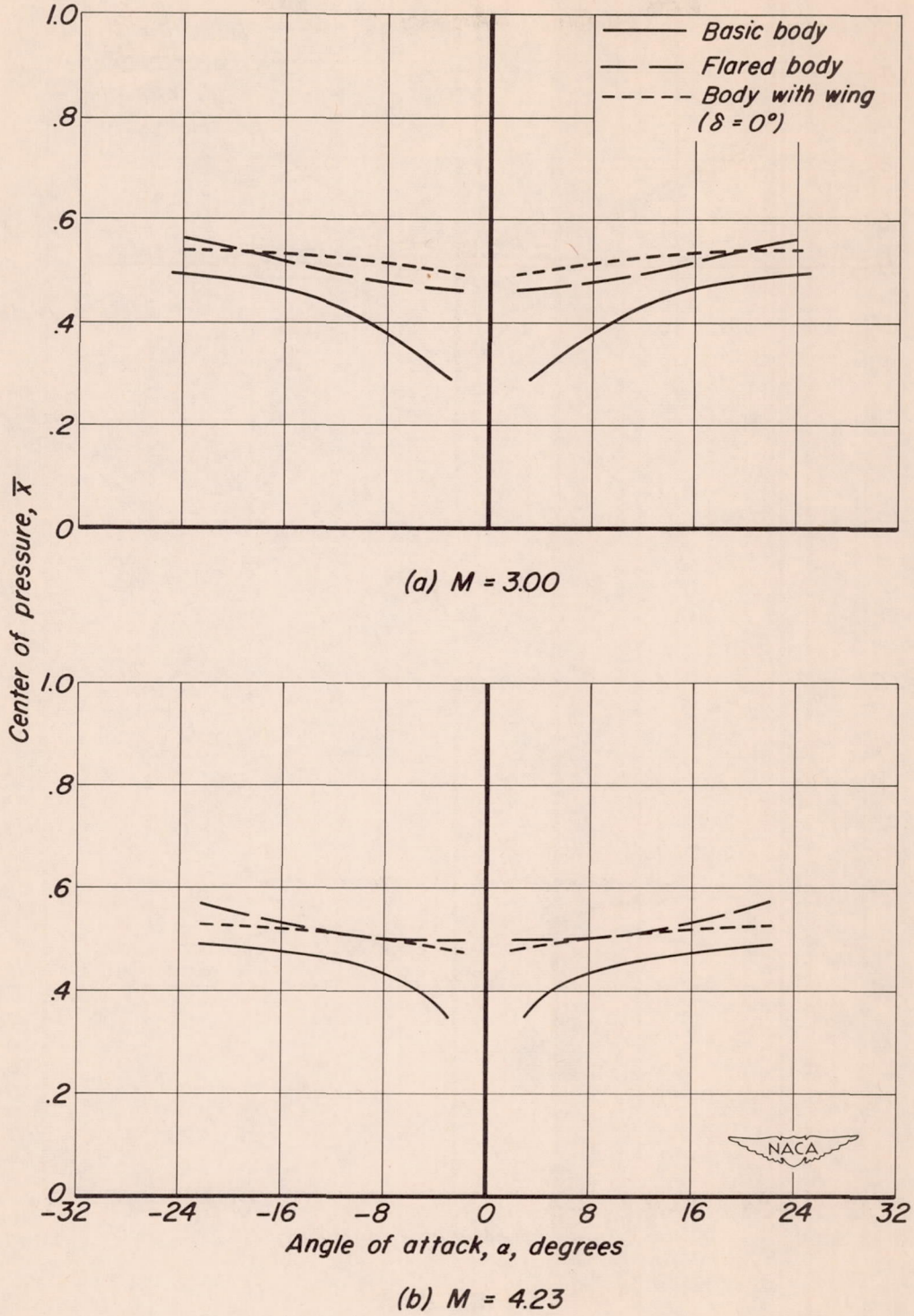

Figure 5.– Variation of center of pressure for basic body, for body with conical flare, and for body with wing.

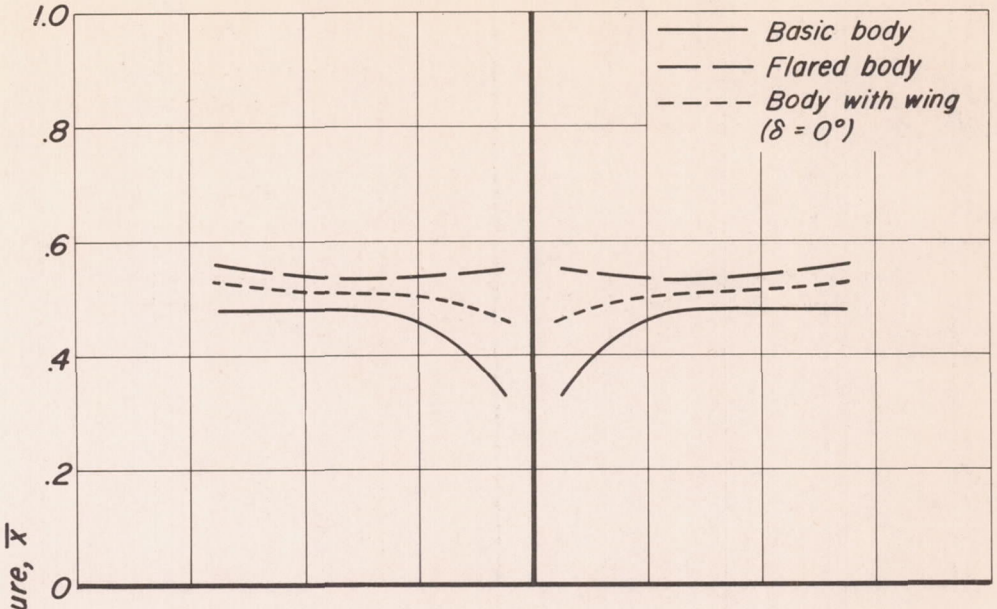

(c) M = 5.05

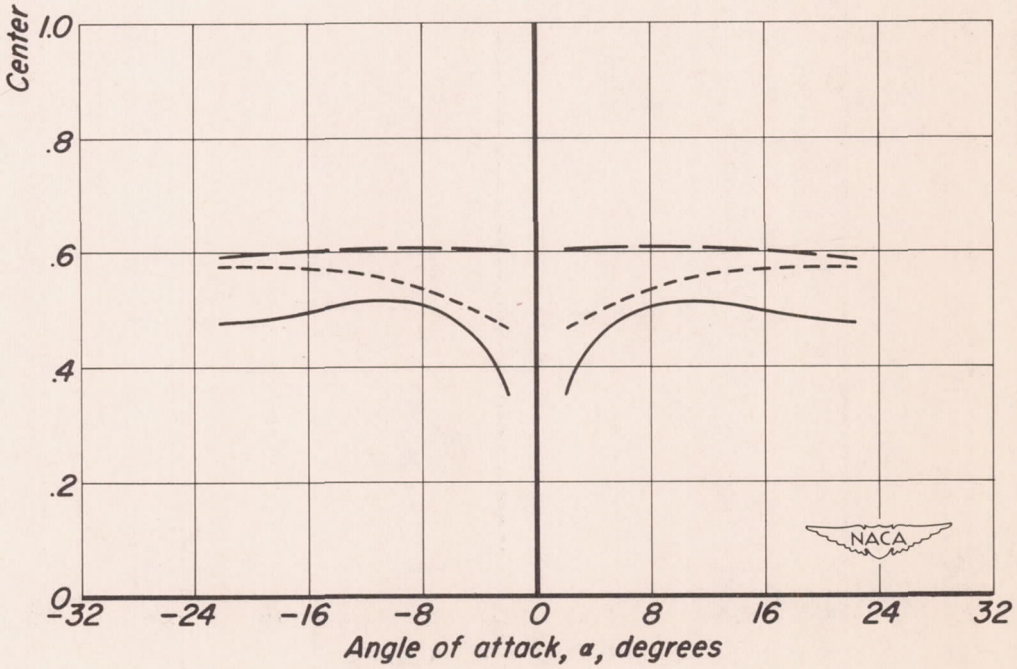

(d) M = 6.25

Figure 5.– Concluded.

DECLASSIFIED

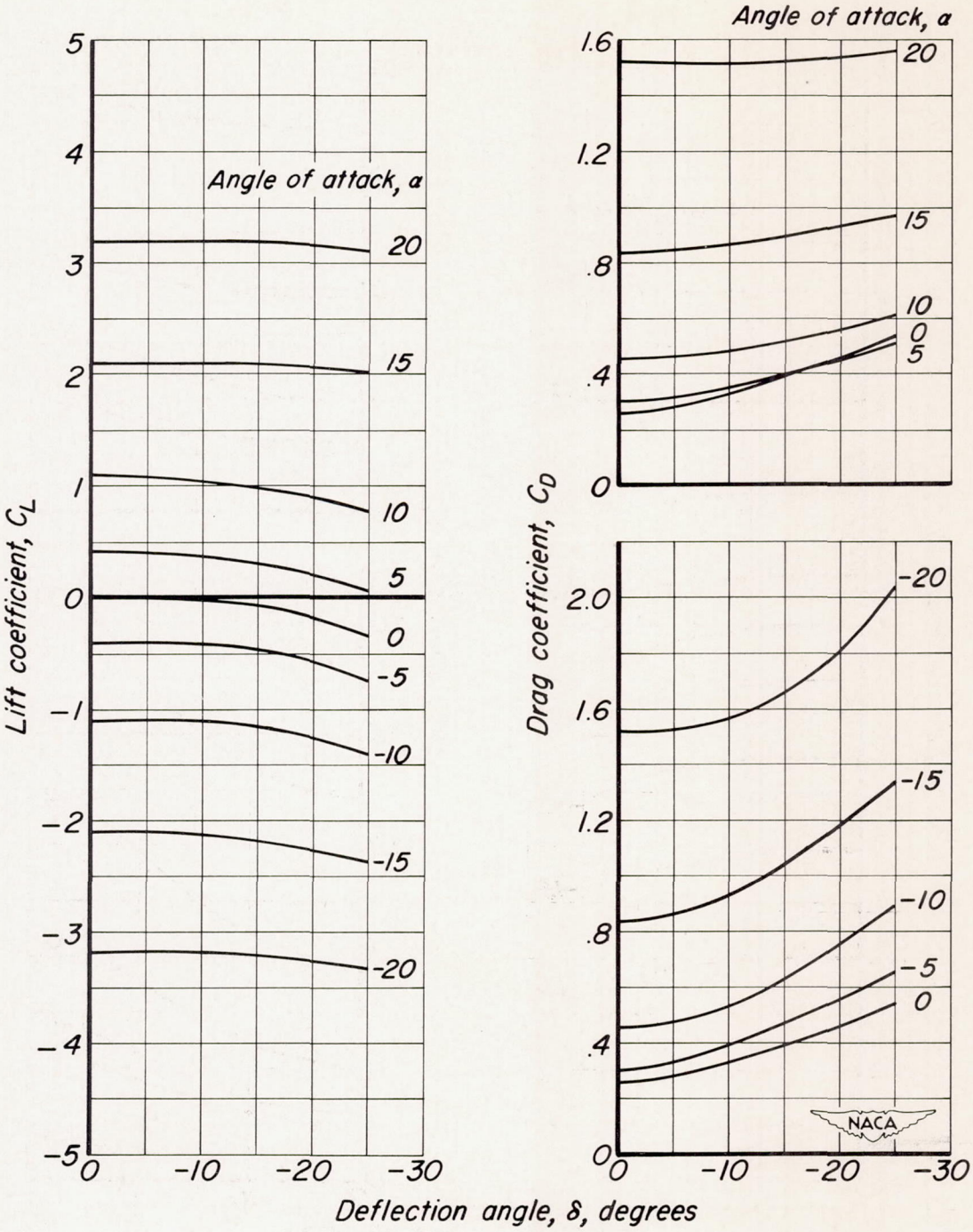

(a) M = 3.00

Figure 6.– Variation of force coefficients with flap deflection.

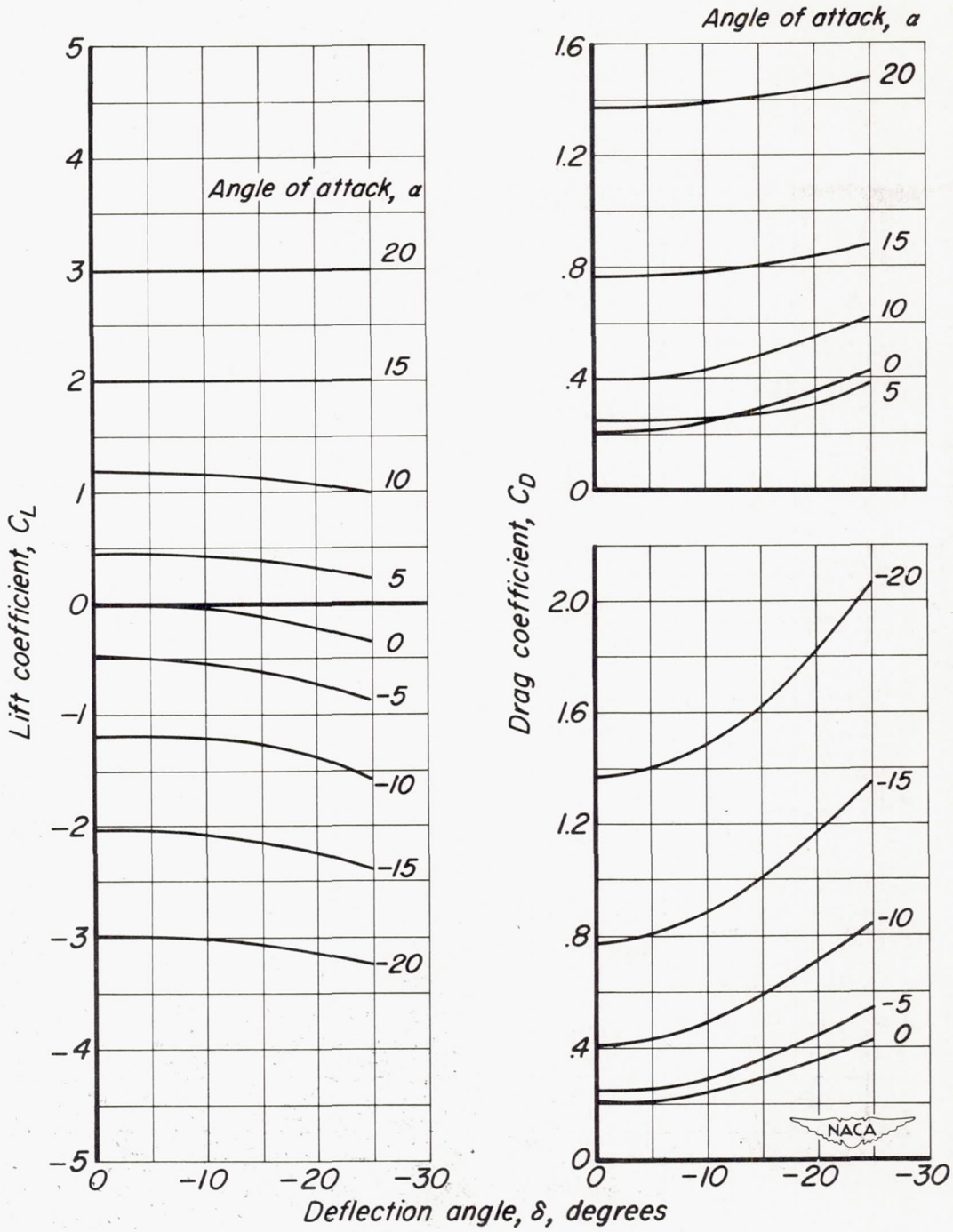

(b) M = 4.23

Figure 6.– Continued.

DECLASSIFIED

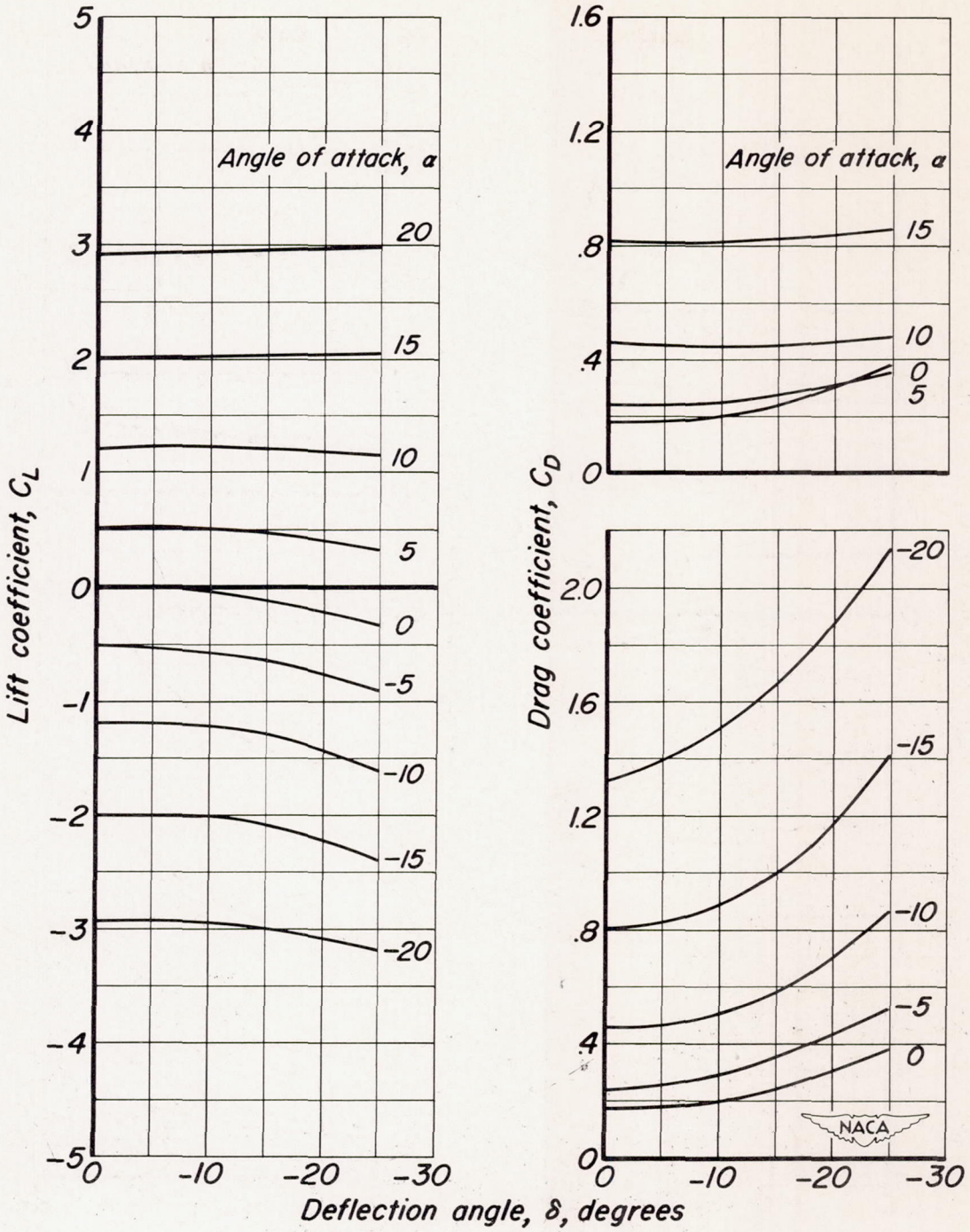

(c) M = 5.05

Figure 6.– Continued.

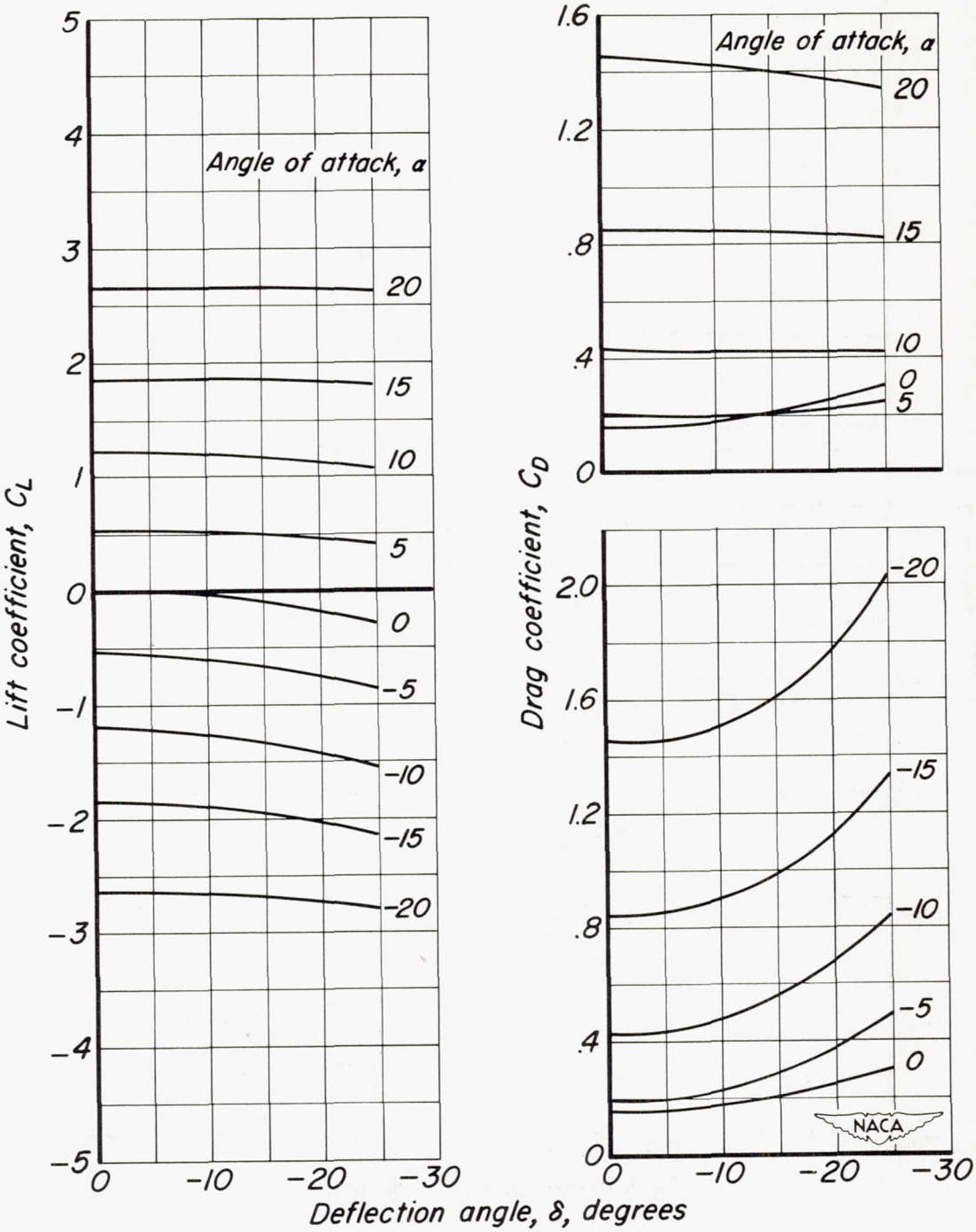

(d) M = 6.25

Figure 6.– Concluded.

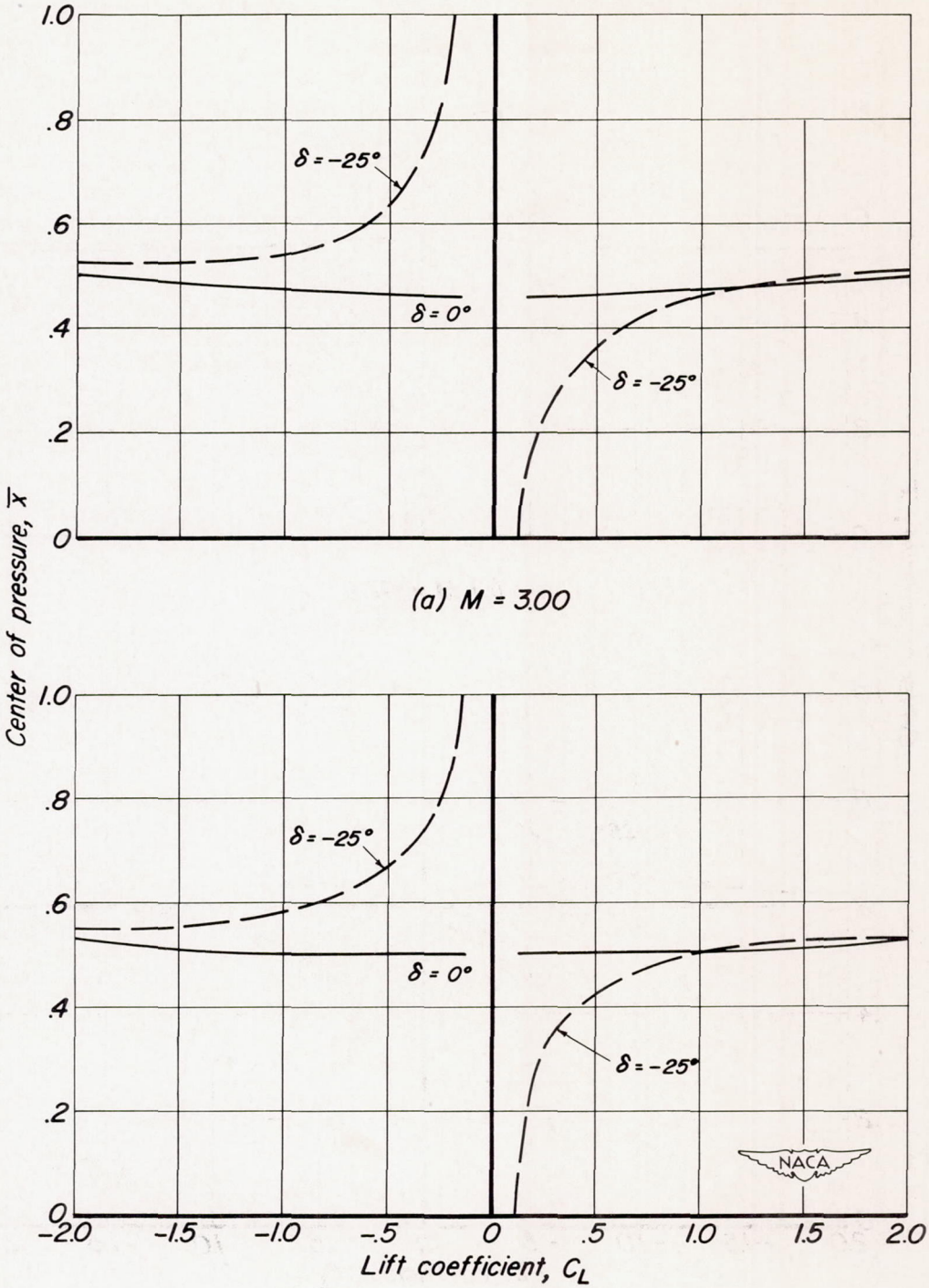

(b) M = 4.23

Figure 7.– Effect of flap deflected −25° on center-of-pressure of body with conical flare.

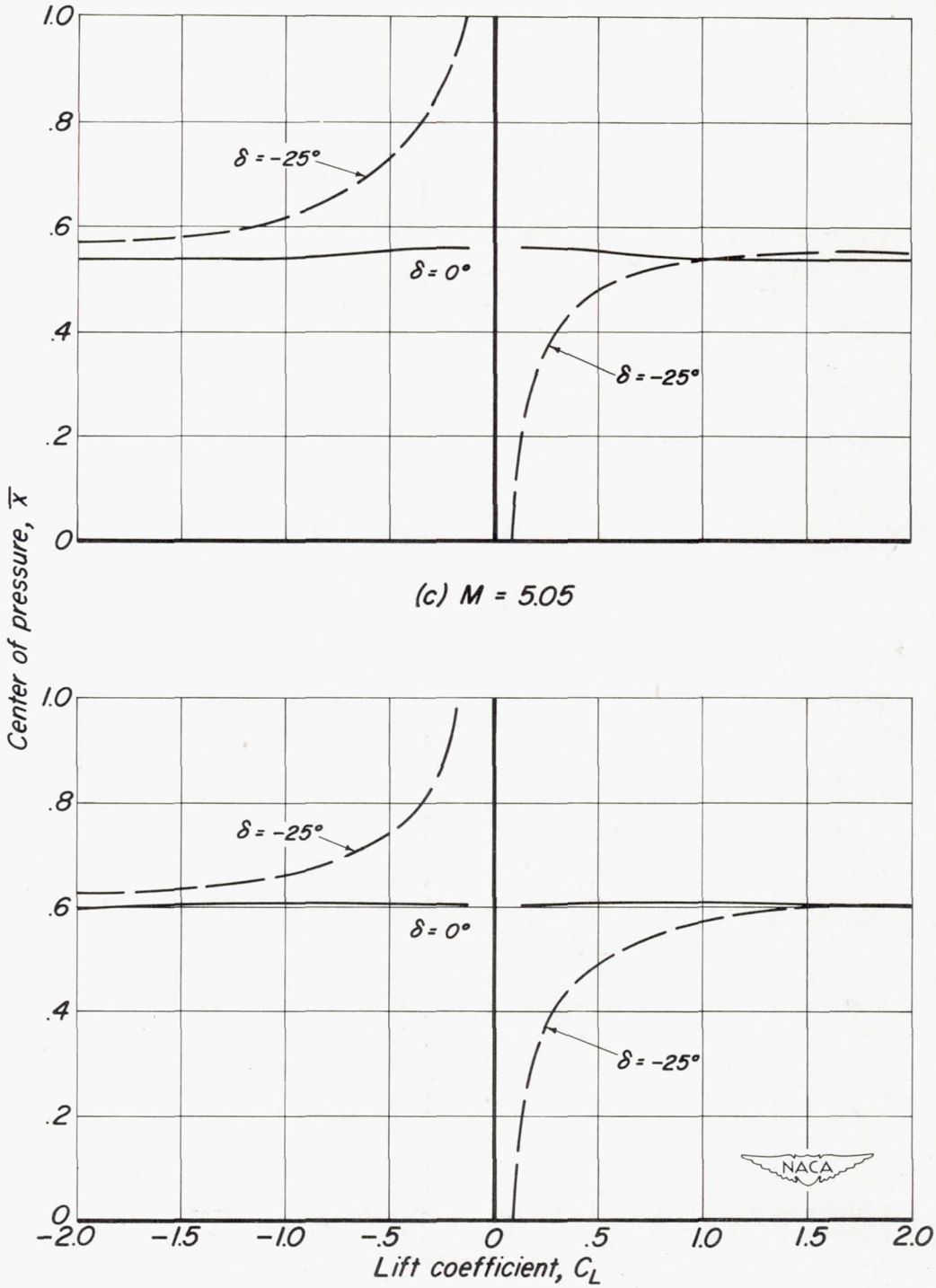

(d) M = 6.25

Figure 7.– Concluded.

DECLASSIFIED

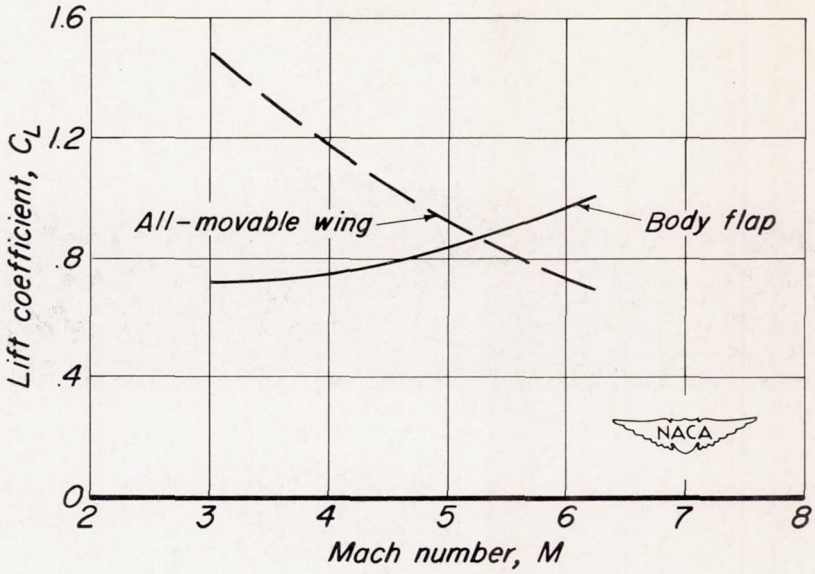

Figure 8.- Trim lift coefficients for body-flap and all-movable-wing models with constant static margin of 3 percent. (Controls deflected −25°.)

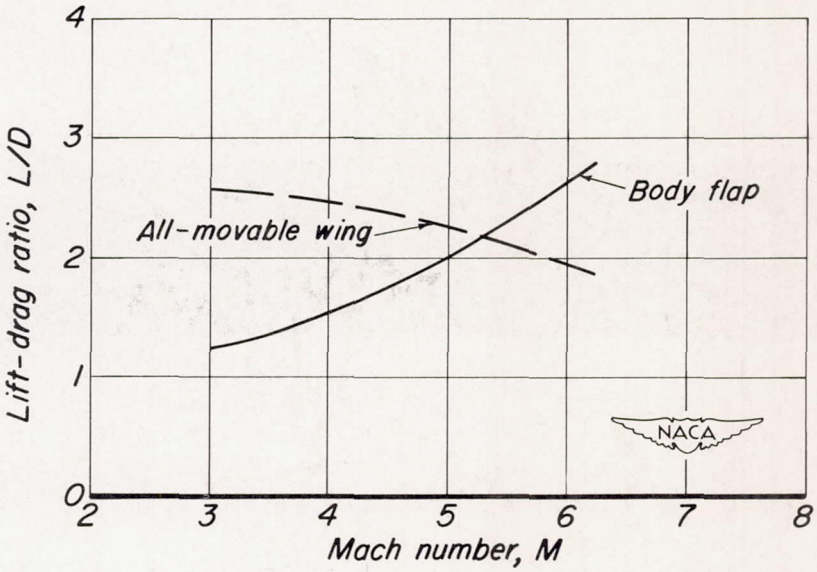

Figure 9.- Trim lift-drag ratios for body-flap and all-movable-wing models with constant static margin of 3 percent. (Controls deflected −25°.)

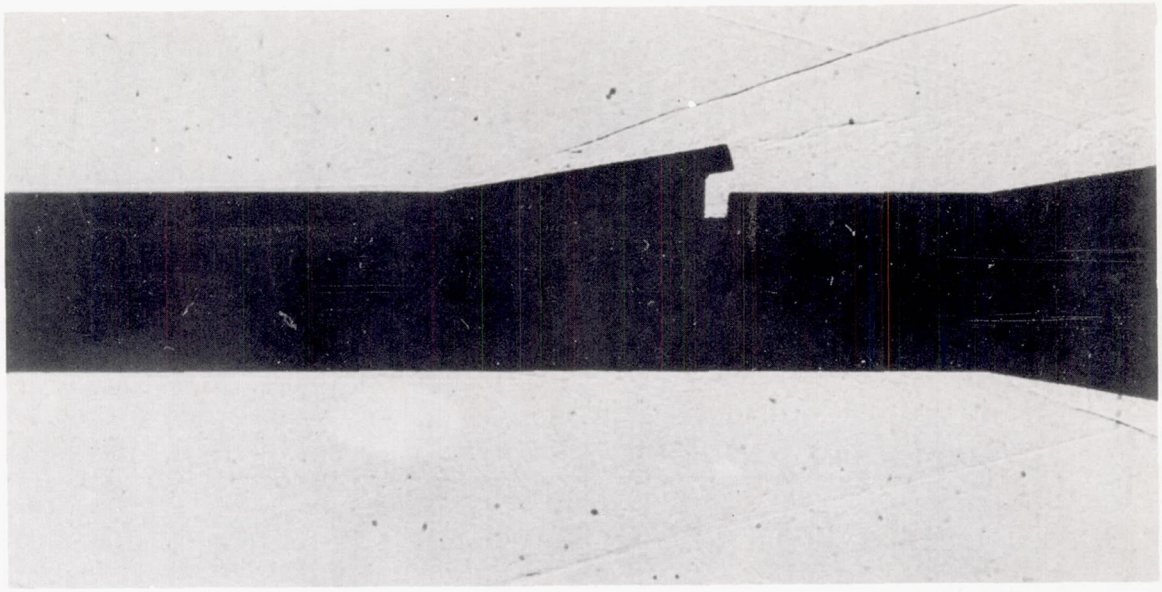

A-19619

(a) Shadowgraph, M = 4.23; $\delta = -10^{\circ}$.

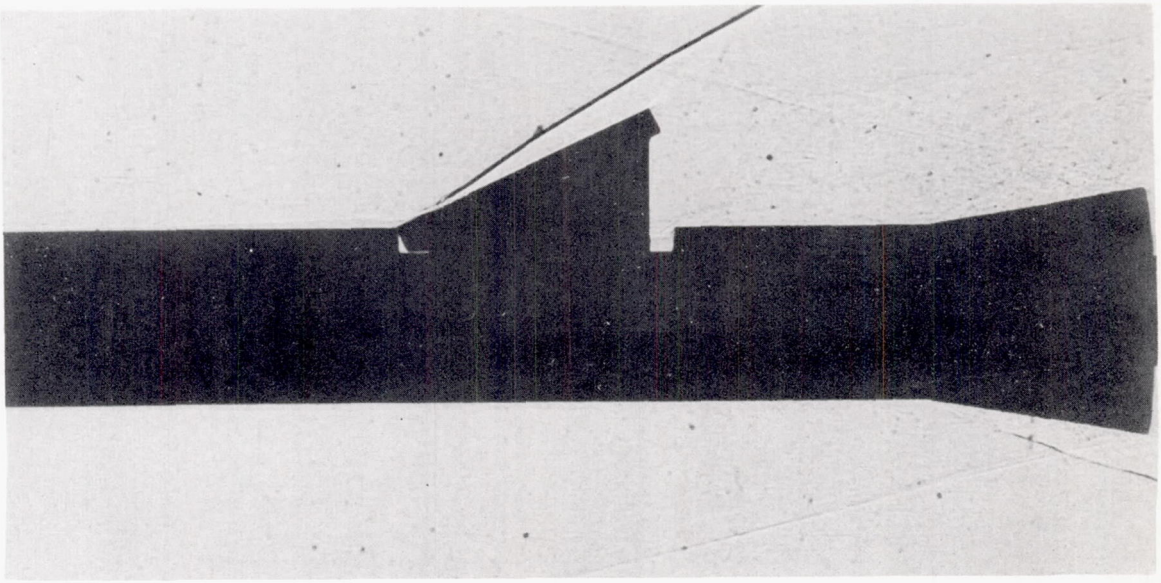

A-19620

(b) Shadowgraph, M = 4.23, $\delta = -25^{\circ}$.

Figure 10.- Flow visualization studies ($\alpha=0^{\circ}$).

DECLASSIFIED

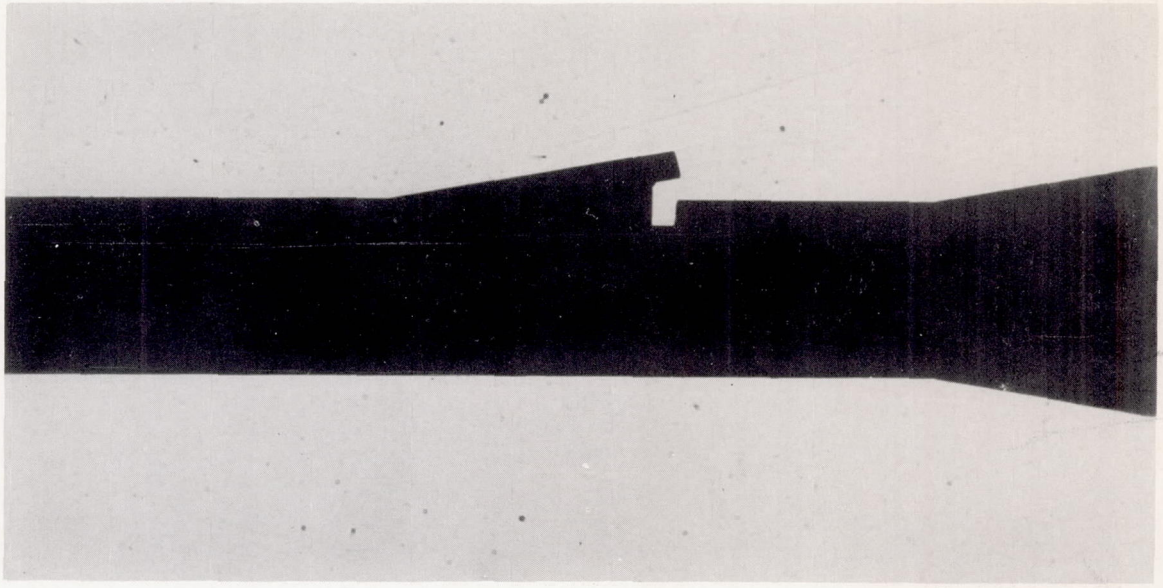

(c) Shadowgraph, M = 5.05; $\delta = -10^{\circ}$. A-19621

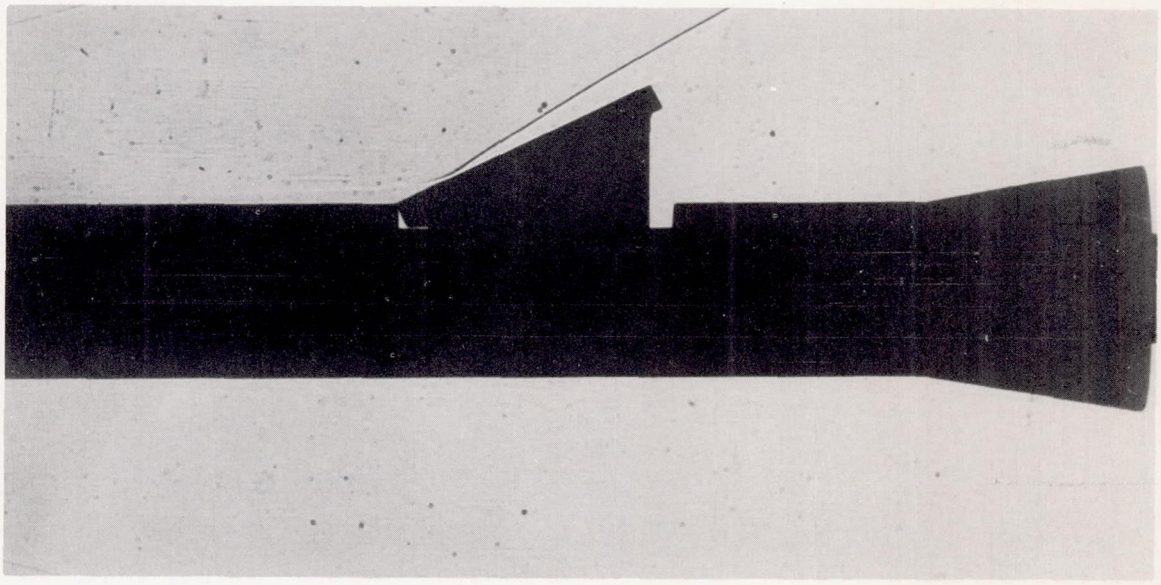

(d) Shadowgraph, M = 5.05; $\delta = -25^{\circ}$. A-19622

Figure 10.- Continued.

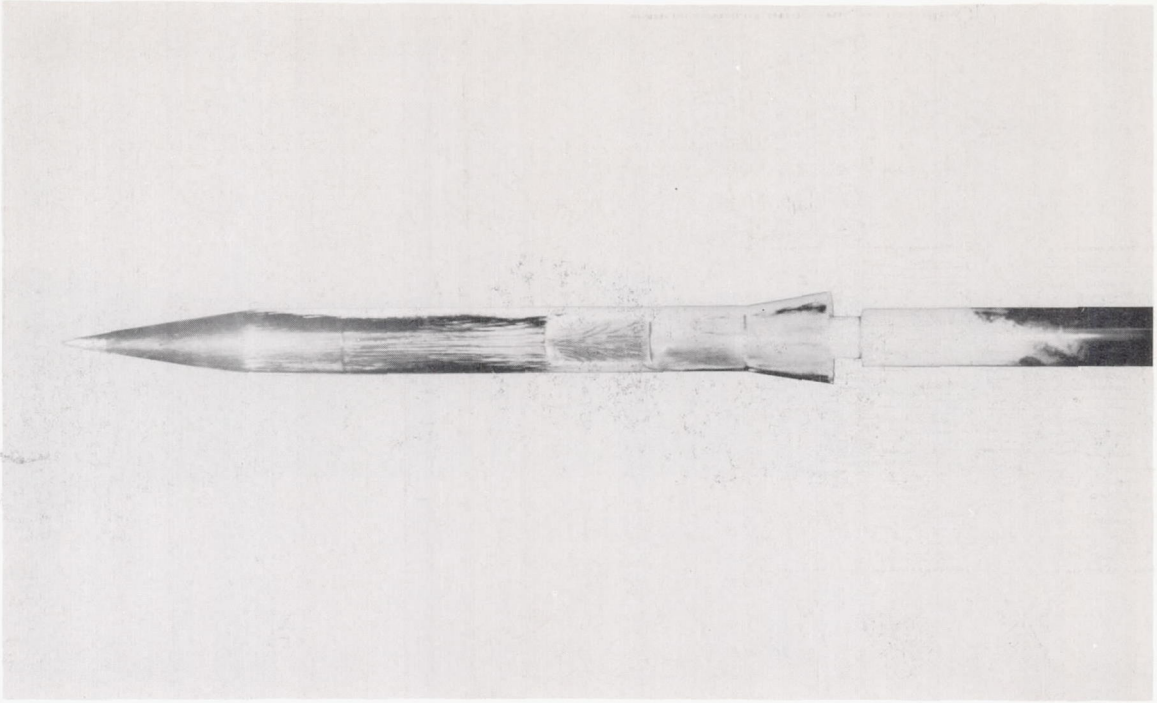

A-19584

(e) China clay, M = 4.23; $\delta = -10^{\circ}$ (top view).

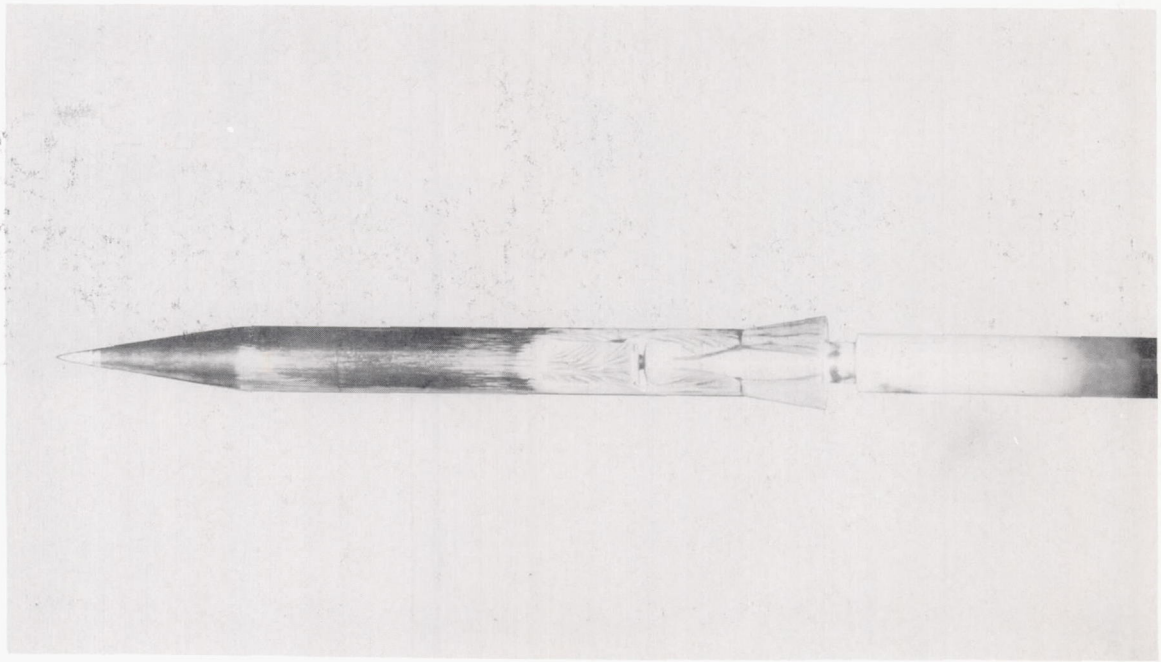

A-19585

(f) China clay, M = 4.23; $\delta = -25^{\circ}$ (top view).

Figure 10.- Concluded.

DECLASSIFIED

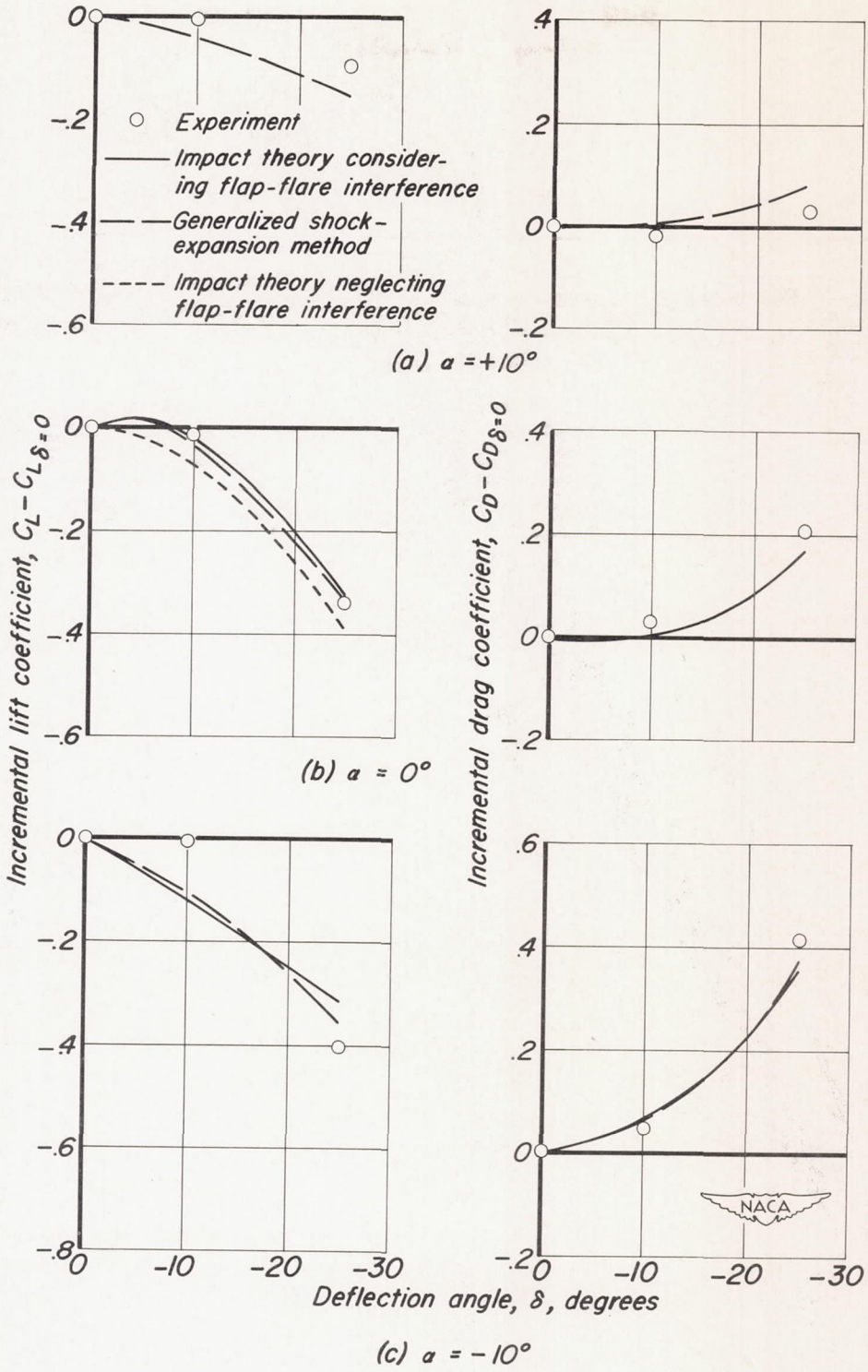

Figure 11.– Comparison between theory and experiment for incremental force coefficients due to flap deflection at a Mach number of 5.05 and several angles of attack.

Figure 12.– Sketch of missile configuration showing proposed body-flap installation.

NACA-Langley - 1-18-55 -350